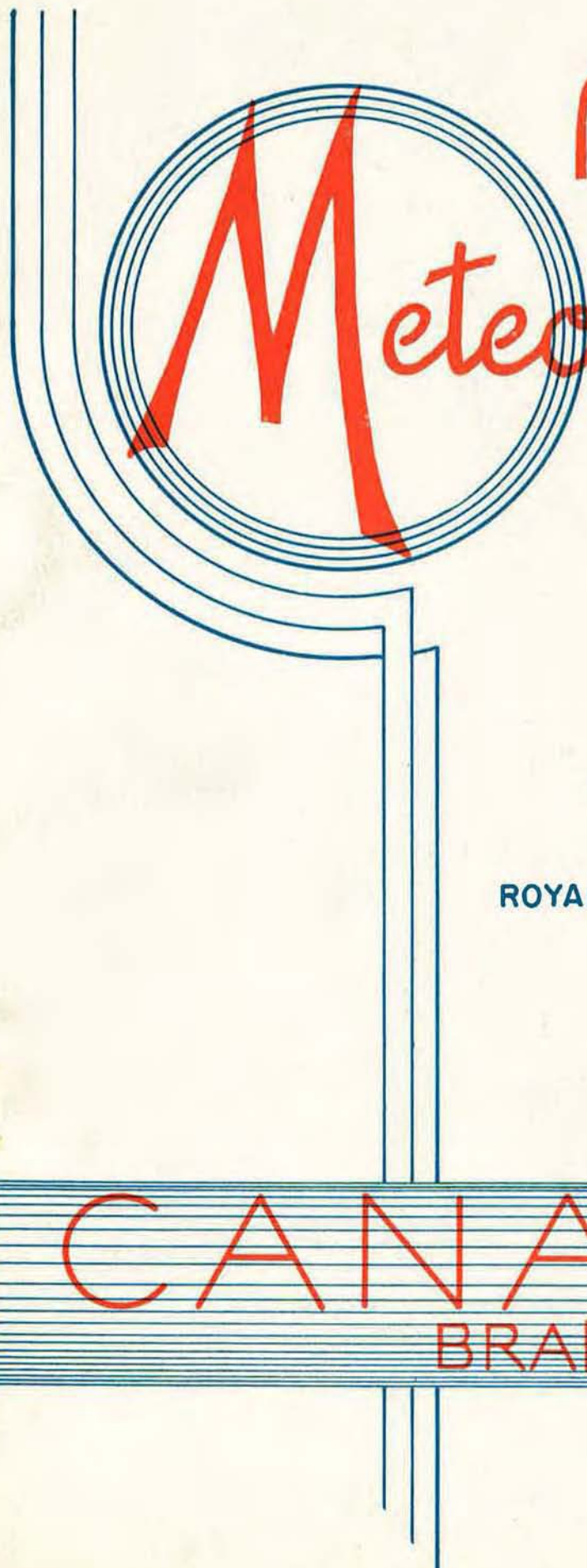


Vol. 7, No. 2.



Royal
Meteorological
Society

PROCEEDINGS of the
Second National Meeting
of the
ROYAL METEOROLOGICAL SOCIETY
Canadian Branch
Toronto, October 18, 1956.

CANADIAN
BRANCH

25¢

Royal Meteorological Society, Canadian Branch

EXECUTIVE COMMITTEE 1956

President R.C. Graham
 Vice-President. Dr. W.L. Godson
 Secretary R. Lee
 Treasurer C.G. Goodbrand
 Councillors-at-large. . . . P. Johns (Montreal)
 S.V.A. Gordon (Winnipeg)
 H. Cameron (Ottawa)
 R.V. Tyner (Vancouver)
 L.B. Foster (Greenwood)
 R.M.S. Vice-President
 for Canada . . . Dr. D. P. McIntyre

Editor. Morley Thomas

Additional copies of this publication are available at a price of 25 cents each. All enquiries and correspondence concerning the Canadian Branch of the Royal Meteorological Society and its publications should be addressed to

The Secretary
Royal Meteorological Society, Canadian Branch
315 Bloor Street West
Toronto 5, Ontario

PROCEEDINGS OF THE SECOND NATIONAL MEETING
OF
THE ROYAL METEOROLOGICAL SOCIETY, CANADIAN BRANCH

Toronto, October 18, 1956.

<u>Contents</u>	<u>Page</u>
1. "Statistics of Extreme Values" by D.W. Boyd and G.R. Kendall, Climatological Division, Meteorological Branch, Toronto	1
2. "Numerical Forecasting on Ferut" by T.J.G. Henry, Research and Training Division, Meteorological Branch, Toronto	13
3. "500 mb Prediction by Graphical Techniques" by B.W. Boville and M. Kwizak, Central Analysis Office, Meteorological Branch, Montreal.	21
4. "Preliminary Report on Ozone Changes 1950-1954 over Edmonton" by E.H. Gowan, University of Alberta, S.J. Buckler and C.E. Thompson, Meteorological Branch, Edmonton	37

STATISTICS OF EXTREME VALUES I

by

D. W. Boyd and G. R. Kendall

Meteorological Branch - Department of Transport - Toronto

1. INTRODUCTION

1.1. The design of any structure is a compromise between making it so strong that it will withstand any stress to which it might be subjected, on the one hand, and building it so cheaply that it is likely to fail, on the other. If the structure is one in which wind stresses are important the designer must choose a design wind, which will be the strongest wind that is likely to occur during the expected life of the structure. The problem of selecting a design wind can only be solved by the use of appropriate statistical methods.

1.2. Stimulated by such problems in climatology and hydrology, the statisticians have done much work in recent years on extreme value theory. The purpose of this circular is to show why special statistics are needed to handle these problems, and to compare the results obtained by the formulae proposed by three writers in this field. No attempt will be made to give the details necessary to use the theories; for this the original papers should be consulted.

2. PROBABILITIES FROM A NORMAL DISTRIBUTION

2.1. A discussion of the distribution of mean temperatures will serve as an introduction, and as a basis for later comparison with the distribution of extremes.

2.2. Table 1 shows the number of years in which the September mean temperature at Quebec City had the values shown.

I Reprinted by permission of the Director of the Meteorological Branch, Department of Transport, from CIR-2825, TEC-238, 9 Oct 1956.

TABLE 1

QUEBEC CITY SEPTEMBER MEAN DAILY TEMPERATURE

<u>Temperature T°F</u>	<u>Number of Years with Temp. T.</u>	<u>Number of Years with Temp. Equal to or Less than T</u>
51	1	1
52	2	3
53	5	8
54	3	11
55	7	18
56	7	25
57	13	38
58	5	43
59	3	46
60	2	48
61	2	50

2.3. Temperatures are given to the nearest degree. Figure 1 shows the numbers of years with temperature T plotted as a histogram, and Figure 2 shows the ogive or the accumulated percentage frequencies. It can be assumed that the probability of a future event is the same as the frequency of the same event in the past. For example, the probability of next September's mean temperature at Quebec City being below 59.5°F. (i.e. 59°F or lower to the nearest degree) is the area to the left of 59.5 in Figure 1 or 92 per cent of the total area. From Figure 2 the value 92 per cent can be read off directly, opposite 59.5°F.

2.4. The irregularities in both figures are due to the fact that we are dealing with a comparatively small number of years. This suggests fitting a smooth curve to the data. If x is the temperature and F(x) the probability that in a given year the mean temperature for Quebec City in September is less than x, then the appropriate equation for the ogive in this case is:

$$F(x) = \frac{1}{\sqrt{2\pi}} \int_{-\infty}^x e^{-\frac{y^2}{2}} dy$$

where $x = \bar{x} + \sigma y$

and \bar{X} and σ are the mean and standard deviation of all the observed mean temperatures. This is the familiar normal or Gaussian frequency distribution, for which tables are available.

2.5. To see how closely the data fit the normal curve the observed accumulated frequencies can be plotted on a frequency scale that is drawn out sufficiently at the ends to make the ogive a straight line. This has been done in Figure 3, using somewhat different plotting positions because the curve is now a continuous function instead of a graph of discrete values. From this curve the probability of September's mean temperature at Quebec City being below 59.5°F . is 93 per cent which is close to the value obtained from the unsmoothed data of Figures 1 and 2.

3. PROBABILITIES FROM AN EXTREME-VALUE DISTRIBUTION

3.1. The original problem of finding a design wind can be made more definite by considering the hourly wind speeds observed at Victoria, B.C., in the years 1923 to 1954 inclusive, a total of 280,512 observations. The problem might be, for example, to find the wind speed which, on the average, will be exceeded only once in the next 50 years or 438,312 hours.

3.2. A frequency curve of the original 32 years' observations would begin at zero wind speed with a fairly large number of calms. It would rise to a mode somewhere near 10 m.p.h. and then drop off, at first fairly rapidly, and then very slowly, finally reaching zero frequency at 69 m.p.h.

3.3. The straightforward approach would be to fit a smooth curve to this distribution (or its ogive) and to determine the wind speed which left an area to the right of only $1/438,312$ of the total. In this method the only part of the curve which would be used would be at the extreme right where the observations are most infrequent and hence the fit poorest. Obviously a method must be devised which gives much more weight to the strongest wind speeds. The method used is to divide the observations into a number of samples (say 32 samples of one year each) and to consider only the largest value from each sample. This is equivalent to using a different variable, namely, the maximum hourly speed recorded each year. The distribution of these annual maxima is referred to as the extreme-value distribution and that of the original set of observations of hourly speeds as the parent population.

3.4. If $F(x)$ is the probability that a value from the parent population is less than x , then the probability that the greatest value (and, therefore, all values) in a sample of n (drawn from the parent population) is less than x is:

$$F^n(x)$$

This is the ogive of the extreme-value distribution for sample of size n . This ordinarily depends on $F(x)$, the ogive of the parent distribution. However, if the variate x is unbounded, if the form of $F(x)$ lies within certain broad limits, and if n approaches infinity, then it has been shown, by E. J. Gumbel (Ref. 1) and others, that the ogive of the extreme value distribution approaches a form which is independent of $F(x)$, namely:

$$G(x) = e^{-e^{-y}}$$

where $x = A + By$.

A and B are parameters analogous to the mean and standard deviation used for normal distributions.

3.5. If this ogive is plotted on a frequency scale that is drawn out suitably at the ends, it can be reduced to a straight line, as was done above with the normal ogive.

3.6. Table 2 shows the number of years in which the maximum hourly wind speed at Victoria had the values shown.

TABLE 2

VICTORIA ANNUAL MAXIMUM WIND SPEEDS

<u>Wind Speed</u> <u>V mi./hr.</u>	<u>Number of Years</u> <u>with Speed V</u>	<u>Wind Speed</u> <u>V mi./hr.</u>	<u>Number of Years</u> <u>with Speed V</u>
40	2	52	4
42	2	53	2
43	1	54	1
44	2	57	1
46	3	58	3
47	1	60	1
49	1	65	1
50	3	67	1
51	2	68	1

3.7. Figure 4 shows these wind speeds plotted on the special frequency scale. The straight line marked "Gumbel" was computed using a least squares method suggested by Gumbel.

3.8. In the case of extreme winds there are two of the conditions on which the straight line was computed that are not satisfied; the variate is bounded below at zero wind speed, and the sample size is not infinite. However, a lower bound would not be expected to have much effect on maximum values and the sample size is fairly large (hourly speeds for a year) and hence a fairly good fit would be expected.

3.9. Attempts have been made to modify the equation to obtain an even better fit. H.C.S. Thom (Ref. 2) was concerned about the lower bound at speed zero. He used the equation;

$$G(x) = e^{-c - y}$$

where $x = A - B y$

which was found by Fisher and Tippett to be the limiting extreme value distribution for variates bounded below at $y = 0$. Hence, Thom's only assumption is that the samples are sufficiently large.

3.10. A different approach was taken by A. F. Jenkinson (Ref. 3). He found that by setting,

$$x = a (1 - e^{-ky})$$

where ak is positive, then the equation

$$G(x) = e^{-e^{-y}}$$

became, in effect, a combination of the three possible limiting equations for x unbounded, bounded above and bounded below. He developed a method of computing a and k from observed data without deciding previously whether the curve in the $x - y$ plane should have positive curvature (bounded above) or negative curvature (bounded below) or zero curvature (unbounded). When

applied to maximum winds it was found that the computed curve had positive curvature. This is the opposite curvature to that assumed by Thom.

3.11. Thom's and Jenkinson's methods were used on the Victoria data and the computed curves are shown with Gumbel's straight line in Figure 4. The three methods give the following answers to the original question, "What wind speed, on the average, will be exceeded only once in 50 years at Victoria?"

Jenkinson	69 m.p.h.
Gumbel	73 "
Thom	77 "

Which is the best estimate, and what is wrong with the others?

3.12. One difference in the three methods that was not mentioned before is the way in which the curves are fitted to the plotted points. Gumbel uses a method based on least squares. Thom uses the method of maximal likelihood. These are both widely used in statistics. Jenkinson uses a different method based on the standard deviation of the annual maxima and on the standard deviation of the two-year maxima. It is a neat solution but may not be as reliable as the other methods. However, it is doubtful if these differences are large enough to explain the differences in the solutions.

3.13. Returning to the assumptions that were made, it will be remembered that Gumbel assumed an unbounded parent distribution and an infinite sample size. Jenkinson and Thom assumed only the infinite samples, and in the case of maximum wind speeds they obtained results on opposite sides of Gumbel's result. This seems to indicate that the curvature of the graphs in the x-y plane depends more on the sample size than it does on the boundedness of the parent distribution.

3.14. If this is true then Thom was wrong in using a theoretical reason for assigning a downward curvature before he studied the data. Jenkinson's curvature may be the right way, but it is interesting to note that his curvature is far greater in this particular case than that of a parabola fitted to the plotted points in the x-y plane using a least squares method.

3.15. If Thom's method is abandoned then there seems to be no theoretical way of determining the curvature in the x-y plane; any curve that is obtained is merely an empirical solution.

3.16. Even after the form of the equation has been determined there is still the difficulty of finding a suitable method of fitting the equation to the observed values. J. Lieblein (Ref. 4) has suggested an alternative method of fitting the equation used by Gumbel. Lieblein's method applied to the Victoria wind data yield a 50-year-return period value of over 3 m.p.h. lower than Gumbel's.

4. CONCLUSION.

4.1. To sum up, - the different methods of predicting extreme values that have been examined give rather widely differing results. None of the methods is completely satisfactory for small samples, but it appears that there is little reason for preferring the methods of Thom or Jenkinson to the more straightforward method developed by Gumbel.

ACKNOWLEDGEMENT

Grateful acknowledgement is made to the observers at Quebec City and at Victoria for the long unbroken weather records they have collected. These are two of the few stations in Canada where observations have been taken at essentially the same location for so many years.

REFERENCES

1. Gumbel, Emil J.
Statistical Theory of Extreme Values and Some Practical Applications.
National Bureau of Standards Applied Mathematics
Series, 33. Washington, Feb. 1954.
2. Thom, H. C. S.
Frequency of Maximum Wind Speeds.
Proceedings, American Society of Civil Engineers
Vol. 80, Separate No. 539, Nov. 1954.
3. Jenkinson, A. F.
The Frequency Distribution of the Annual Maximum (or Minimum)
Values of Meteorological Elements.
Quarterly Journal, Royal Meteorological Society
Vol. 81, No. 348, p. 158, Apr. 1955.
4. Lieblein, Julius
A New Method of Analyzing Extreme-value Data.
National Advisory Committee for Aeronautics
Tech. Note 3053 Washington, Jan. 1954.
5. Meteorological Division
The weather data used as examples were taken from abstracts on
file at the Climatological Office. Most of the data have been
published in the Monthly Record.

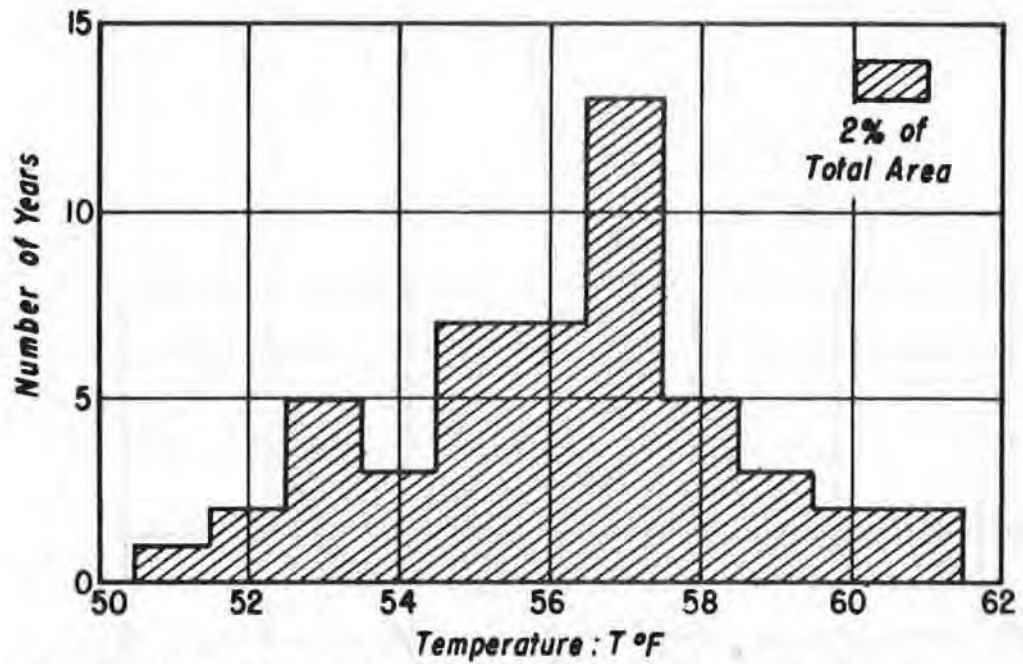


Fig. 1. Histogram of September Mean Temperatures at Quebec

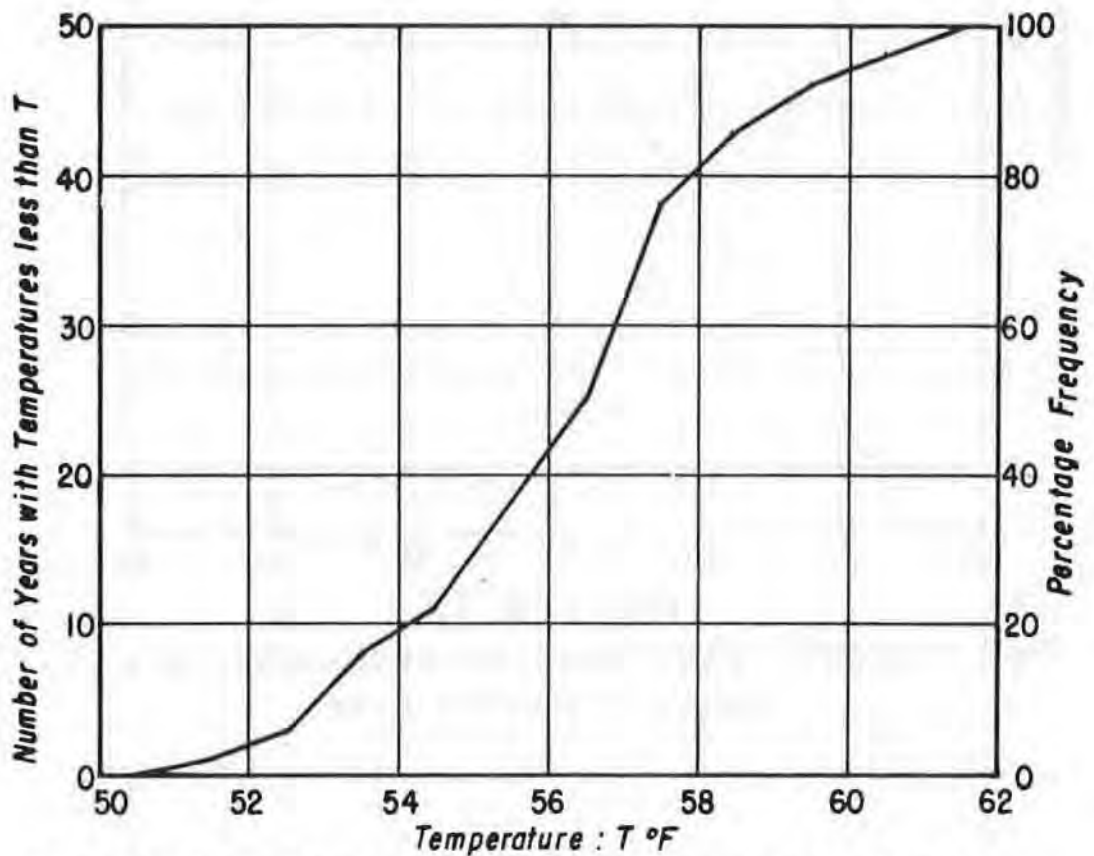


Fig. 2. Ogive of September Mean Temperature at Quebec

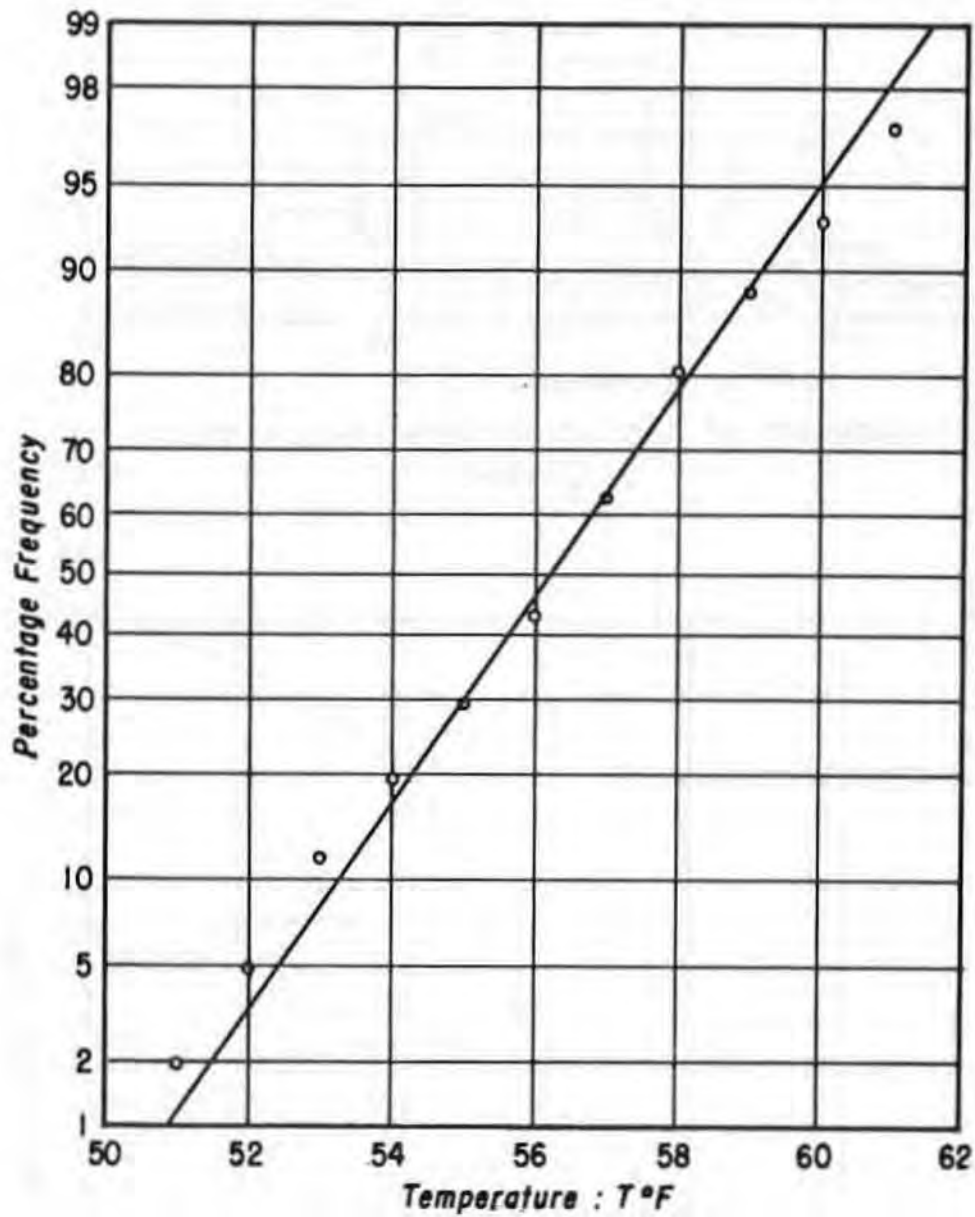


Fig.3. September Mean Temperatures at Quebec on a Normal Probability Scale

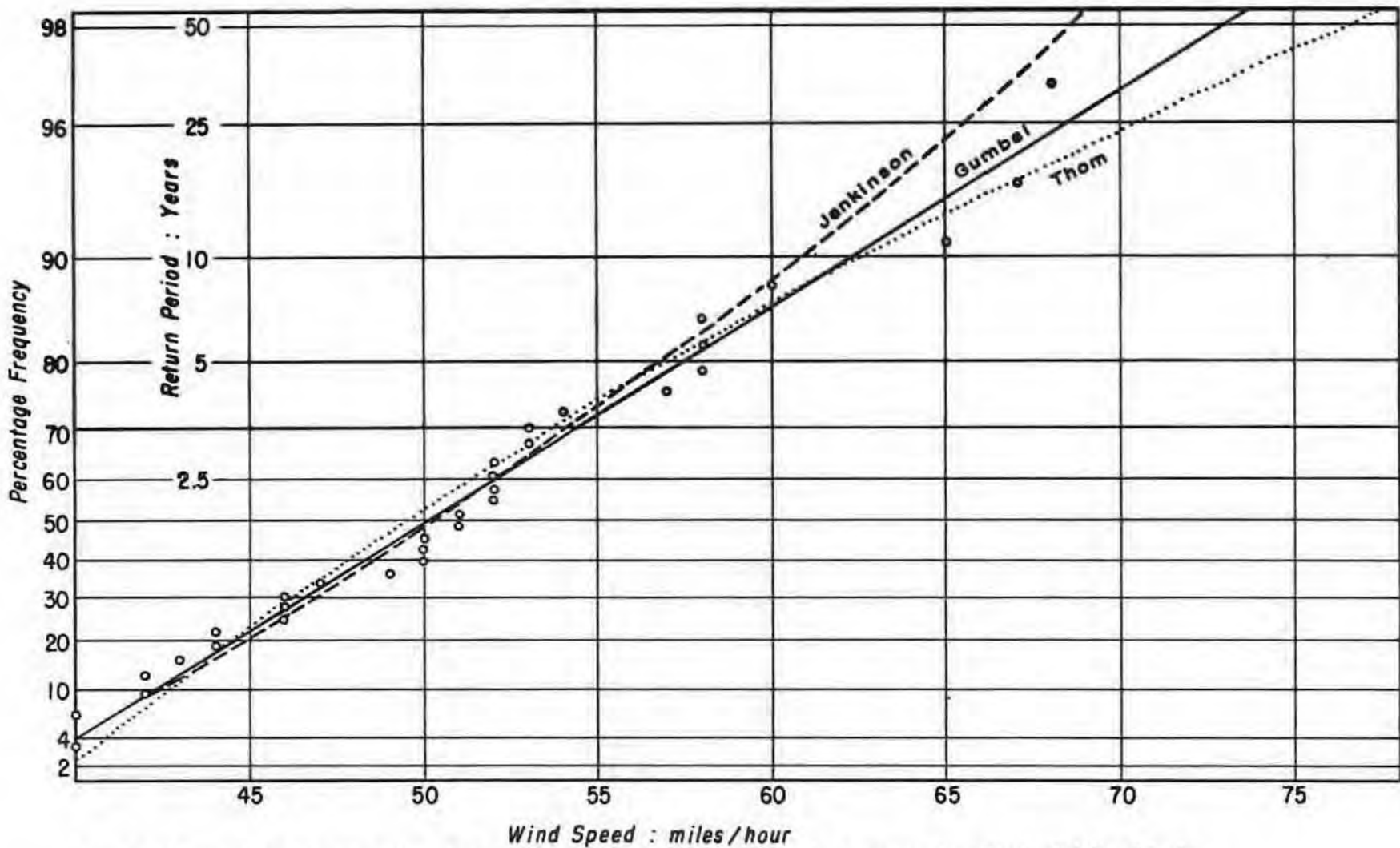


Fig. 4: Annual Maximum Wind Speeds at Victoria on an Extreme-value Probability Scale.

(blank page)

NUMERICAL FORECASTING ON FERUT

by

T.J.G. Henry

Meteorological Branch, Department of Transport - Toronto

The physical laws governing the motion of the atmosphere have been fairly well understood for many years. Consequently, there has existed the theoretical possibility of integrating the basic equations step by step to determine the fields of motion, pressure and temperature at future times. Until recently, the amount of computation involved in this process has been prohibitive. With the advent of high-speed electronic computers, however, the computation problem has become somewhat more tractable. Although developments in this field are still at a rather early stage, numerical forecasting with the aid of electronic computer equipment is already an operational reality in the United States and Sweden, and is scheduled to go into operational use in the United Kingdom in the near future.

Most attempts at numerical forecasting to date have involved the use of an atmospheric model, in which the pressure and wind fields at all levels are inferred from those at one or more key levels. The simplest type of model is a one-parameter model, in which the wind flow at each level is assumed to be parallel in direction and proportional in speed to the wind at some standard level, which is usually taken to be the 500-millibar level. In one version of this model, vorticity and advection are calculated on the assumption that winds are geostrophic and may be inferred from the 500-mb height pattern. More complicated models use two or more parameters to represent the variation of the wind field in the vertical. For example, the "thermotropic" model recently introduced by the Joint Numerical Weather Prediction Unit in Washington is a two-parameter model in which the wind flow at each level is inferred from the height patterns at two standard levels, the 500-mb level and the 1000-mb level. Models with more than one parameter permit a better representation of the flow patterns at different levels, and make it possible to forecast the patterns of temperature and vertical motion as well as the patterns of pressure and wind flow for one level.

After a good deal of preliminary study, the Meteorological Division has begun development work in the field of numerical forecasting, using the Ferranti Mark I electronic computer at the University of Toronto (FERUT). Up to the present time, progress has been rather slow, mainly because it takes a good deal of time for a newcomer to the art of automatic computation to acquire proficiency in programming operations of this kind for an electronic computer. However, it is expected that future progress will be more rapid.

FERUT is a large-scale stored-program computer operating in the binary system. This system is used inside the computer in preference to the more familiar decimal system because it is easier to engineer. Conversion of numerical data from decimal to binary form during input, and from binary to decimal during output, are carried out at full speed by means of standard routines permanently stored in the computer. Numbers and instructions are represented inside the computer as rows of binary digits or "bits". Numbers can be stored either as "long lines" of 40 bits (equivalent to 11-12 decimal digits) or as "short lines" of 20 bits (equivalent to 5-6 decimal digits.) The latter scheme is used in numerical forecasting. Each instruction consists of 20 bits. These include 6 operation digits, which specify the type of operation to be carried out; 9 address digits, which specify the storage location containing the number to be operated on; 3 modifier digits, which specify one of 8 auxiliary registers that may be used to modify the instruction; and 2 spare digits that are not used. The storage unit or memory consists of two parts, a magnetic drum of large capacity and a rapid-access or working store composed of 8 cathode-ray tubes, each capable of storing 64 20-bit lines. For input and output ordinary 5-hole paper teletype tape is normally used, but equipment is also available for using IBM punched cards.

The first experimental forecasts on FERUT have been made with a one-parameter model, in which the motion at all levels is inferred from the geostrophic wind at 500 mb. These assumptions lead to a Poisson equation for the local 500-mb height tendency, of the form

$$\nabla^2 \frac{\partial z}{\partial t} = F(x, y, t).$$

In this equation, z is the 500-mb height at any point on the map at time t , and ∇^2 is the two-dimensional Laplacian operator $\frac{\partial^2}{\partial x^2} + \frac{\partial^2}{\partial y^2}$.

The quantity F involves the advection of absolute vorticity with the wind. The wind and the absolute vorticity η are both evaluated geostrophically from the 500-mb height distribution. The equations used are:

$$\eta = \frac{gm^2}{f} \nabla^2 z + f,$$

$$F = \frac{\partial \eta}{\partial x} \frac{\partial z}{\partial y} - \frac{\partial \eta}{\partial y} \frac{\partial z}{\partial x},$$

where g is the acceleration of gravity, f is the Coriolis parameter and m is the local map scale. By solving the Poisson equation for $\partial z / \partial t$ we can obtain the 500-mb height tendency at each point on the map.

For solution on an automatic computer, equations involving derivatives have to be replaced by finite-difference approximations. Thus, gradients of height or vorticity are replaced by differences

between neighboring points of a rectangular grid, and the forecast period is divided up into a series of finite time steps. This use of finite time and space intervals introduces truncation errors which make it impossible to forecast accurately the motion of small-scale features whose geographical extent is comparable to the distance between successive grid points. Moreover, the time step Δt must be chosen sufficiently short that the distance the air moves during one time step is everywhere small compared to the grid interval. Centred space and time differences are used wherever possible. The finite-difference Poisson equation for the 500-mb height tendency $\partial z / \partial t$ is solved by an iterative process due to Richardson and Liebmann. For each grid point, the value of z for time $t + \Delta t$ is then obtained from the value of z at time $t - \Delta t$ by adding $\frac{\partial z}{\partial t} 2 \Delta t$, where $\partial z / \partial t$ is evaluated for time t . This gives us a new 500-mb height distribution, and by repeating this process over a sufficient number of time steps we obtain a 500-mb prognostic chart for any given time in the future.

So far, we have made one set of full-scale production runs with this model. The initial 500-mb map for these runs was for 0300 GMT March 13, 1955, and is shown at the upper left in Fig. 1. Initial 500-mb heights were read off for a grid of 15 rows and 19 columns centred at 55°N , 95°W , with a grid spacing of about 175 miles. In most of the runs, the heights on the grid boundary were assumed to change linearly with time at such a rate as to reproduce the 24-hour changes that actually occurred. In actual forecasting, these changes would of course not be known in advance, and would have to be forecast in some manner. For this first test, we thought we had better concentrate on the interior of the grid and come back to the problem of boundary conditions later. The actual map for 0300 GMT March 14, 24 hours after the time of the initial map, is shown at the upper right.

In the first run, a time step of one hour was used, and three iterations were used in solving the Poisson equation in each time step. The 24-hour forecast map is shown at the lower left. It will be seen that agreement is generally good for the eastern half of the chart; for example, the motion of the centre of low in Maine is forecast quite well. Over the Plateau region in the west a marked trough and centre of low height were forecast to develop, but this prediction did not verify. This failure is probably due to inadequacies of the simple model used, which neglects the effects of topography and of the variation of the streamline patterns with height. Errors near the upper boundary of the grid are probably due, at least in part, to the assumption of linear height changes with time on the boundary. Actually, a centre of low moved slowly southward across the grid boundary, so that the heights first fell and then rose.

The second run used a time step of $1\frac{1}{2}$ hours instead of one hour, and the third run used five iterations to solve the Poisson equation in each time step instead of three. In both cases the forecast charts were practically identical with those obtained in the first run.

In the fourth run, the 500-mb heights on the grid boundary were held constant during the forecast period. This scheme was tried out because it is one of several completely objective procedures that could be used in operational forecasting, without introducing a subjective forecast for the boundary points. In this case the quality of the forecast was considerably reduced, as may be seen from the resulting map shown at the lower right. In particular, the spurious troughing over the Plateau was intensified. The effect of the boundary conditions would probably vary a good deal from one case to another, but for a small grid like the one used here, the effect is clearly important.

With this grid of 19 x 15 points, the machine time used for a 24-hour forecast in one-hour steps, using 3 iterations to solve the Poisson equation in each time step, was 43 minutes. This includes about 5 minutes for reading in the program and the data and 12 minutes for punching out the forecast 500-mb heights at 6-hour intervals (3 minutes each time). The actual forecast cycle took about 1 minute and 10 seconds per time step. On a very fast computer, such as the IBM 701 used by the Joint Numerical Prediction Unit in Washington, the time for a 24-hour forecast with this model and grid size would probably be between 5 and 10 minutes.

This first group of experimental forecasts has given us valuable experience, but much further work remains to be done. We particularly wish to follow up various advances that have been made by the U.S. groups in Washington and Princeton, by the British Meteorological Office and by the group headed by Professor Rossby at the University of Stockholm.

In order to minimize boundary effects, it will undoubtedly be necessary to use a grid covering a larger area. A one-parameter (barotropic) forecast over a large area can be made without a prohibitive expenditure of machine time. Moreover, certain improvements in the computation scheme have been reported on by the Princeton and Stockholm groups and are now being used operationally by the U.S. Numerical Prediction Unit. By avoiding the use of the geostrophic assumption, this new scheme eliminates certain types of systematic error that were noticed in the earlier barotropic forecasts.

The Washington group has recently introduced a two-parameter thermotropic model which incorporates the effects of topography and vertical motion. Programming of a model of this type for FERUT is now nearly completed. Limitations of storage space have made it necessary to use a rather small grid, of the same size as was used in the first one-parameter forecasts, in order to obtain a reasonably efficient computation scheme. However, it is hoped that some useful experience can be gained.

Rather simple graphical procedures for numerical forecasting have been suggested by Fjörtoft, Estoque and others. These procedures can be adapted for machine computation. It will probably not be feasible to advect perturbations in steps of 12 or 24 hours as can be done graphically, but even so, it seems probable that a rather

fast computation scheme can be devised, and we hope to try out one or two forecasts on FERUT using these techniques.

Both the Washington group and the Stockholm group have done considerable work on the problem of objective analysis from station reports of height and wind for a given isobaric surface. Operational techniques have been developed for interpolating the heights at grid points directly from such reports. A scheme of this sort is probably essential to the effective use of a computer in forecasting, but it makes rather heavy demands on the storage capacity of the computer. It is not yet clear whether it would be profitable for us to attempt development work on this problem on FERUT, or whether we should leave this work to other groups having access to a larger computer. If the prospects of doing useful work appear to be reasonably good we may try it.

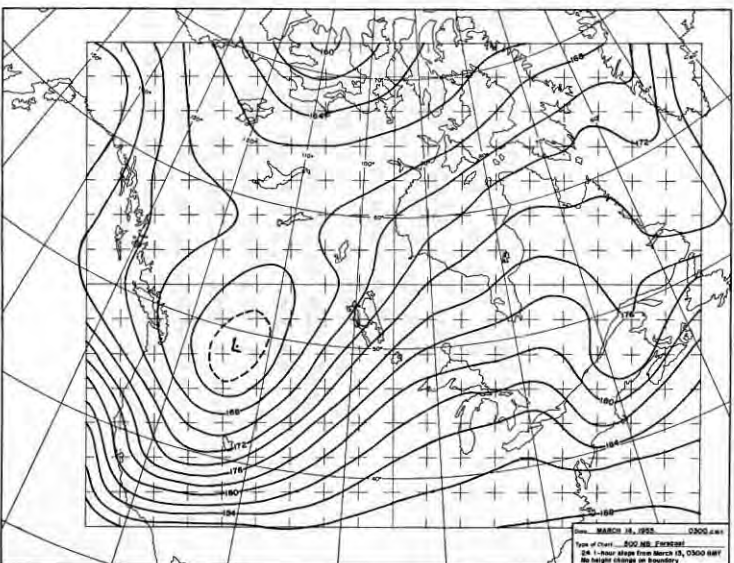
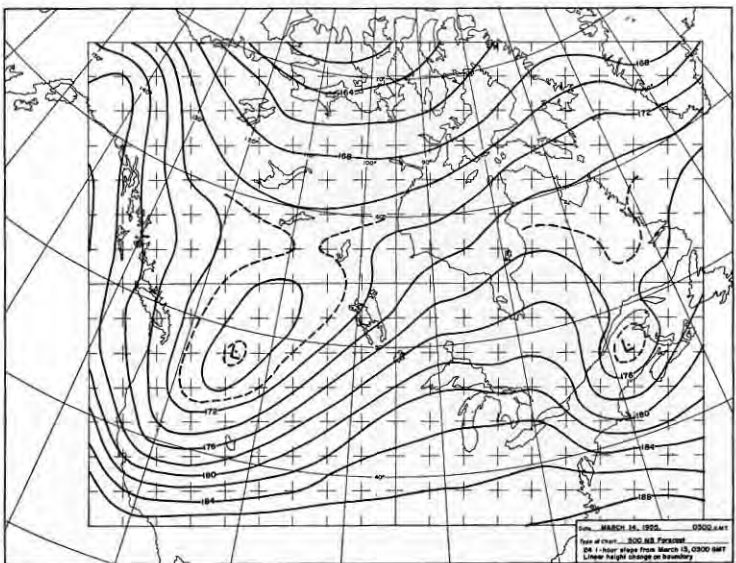
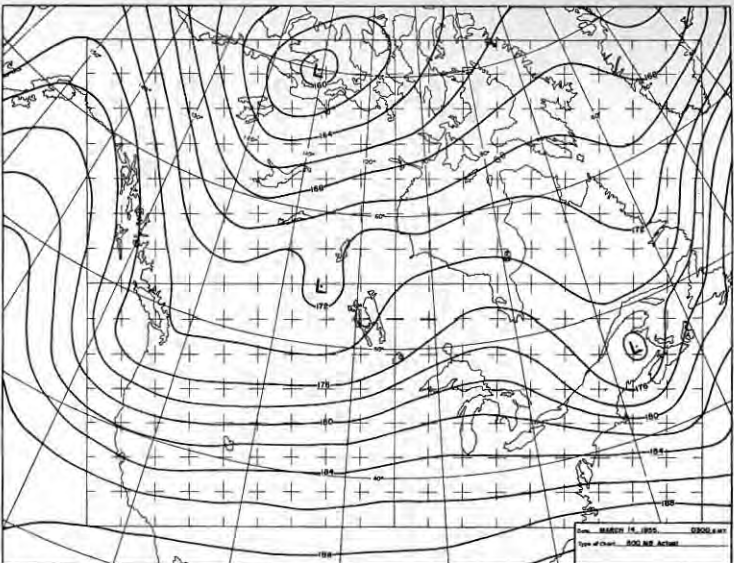
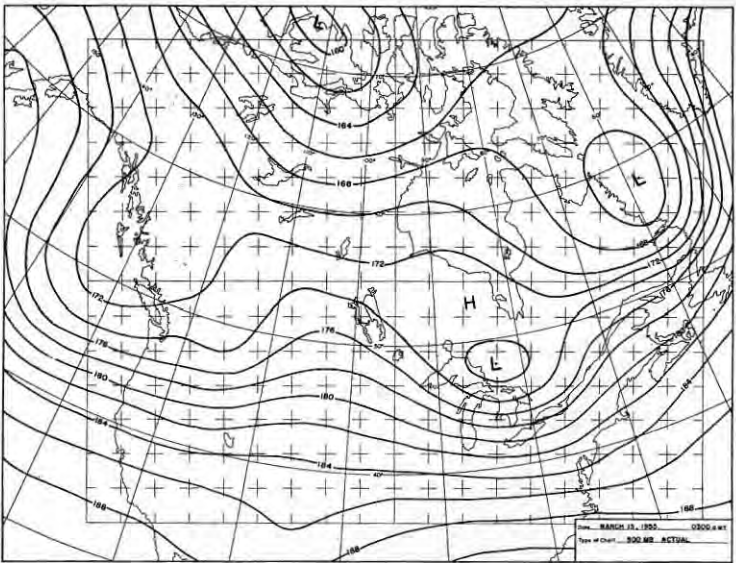
It will be evident from this outline of the experimental work that has been done on FERUT that we have made only a very small beginning, and have a long way to go to overtake the progress that has been made in other countries. The question naturally arises, whether it is ever likely to be an economic proposition for the Meteorological Division to go into numerical forecasting on a computer as a routine operation; in other words, can numerical forecasting ever be sufficiently useful to justify the very considerable cost of acquiring a computer or using one on a part-time basis?

Any forecast of the future role of electronic computation in Canadian meteorology must be based, not on the crude results presented here, but on what has already been done in the United States and Sweden, where advanced techniques have been in operational use. On this basis, I believe it can be expected that computers will be able to do some jobs in forecasting better than they are now done by meteorologists, and will open up lines of advance in areas where little progress is now being made. If this happens, considerable economic benefits may be realized from types of forecasting that can now be done with only marginal success. It seems unlikely that forecasters can ever be replaced by machines to any appreciable extent. They will still be needed to do the essential job of any forecast service, namely the detailed forecasting of actual weather and the provision of specialized advice to the transportation industries, to agriculture and to other users of forecasts.

If, then, we view the role of the computer in meteorology as one of assisting the meteorologist to do some jobs better, and of opening up new lines of attack on meteorological problems, my forecast would be that numerical forecasting in Canada with the aid of a computer will eventually be economic. However, careful studies along certain lines will be essential. In the first place, we need to continue development work in the techniques of numerical forecasting, trying out techniques that have been used elsewhere and developing new ones ourselves. In the second place, we need to consider very carefully the characteristics of computation equipment now available or likely to be introduced, and

the sort of equipment that would be required to do the jobs we would want to do in meteorology. In the third place, we need to consider other possible applications of high-speed computation in meteorology besides forecasting, so that any plans for using computer equipment in forecasting can be coordinated with other possible requirements. It is also possible that the Meteorological Division might be able to use a computer in cooperation with other agencies, as the Swedish Air Force Weather Service has done at the University of Stockholm. If we proceed cautiously along these lines, I think electronic computer equipment can eventually make an economically sound contribution to meteorology in Canada.

FIGURE 1



(blank page)

500 MB PREDICTION BY GRAPHICAL TECHNIQUES

by B. W. Boville and M. Kwizak

Meteorological Branch, Department of Transport
MontrealABSTRACT

A graphical technique for 500 mb prognosis based on an extension to Fjörtoft's barotropic model is presented. The propagation of both large scale (of order of 90 degrees) and small scale (of order of 45 degrees) wave systems is accomplished by the use of single and double space smoothing methods. The barotropic equation is developed and the role of the Jacobian operator and the chart magnification are discussed as the basis for numerical models. The graphical solutions for the vorticity and space mean charts and the prediction equation are given. The general applicability of these charts to a prognostic program is discussed briefly and an example of the method is given.

500 MB PREDICTION BY GRAPHICAL TECHNIQUES

by B. W. Boville and M. Kwizak

1. Most meteorologists agree that the day to day variations in the intensity and structure of weather systems must be accounted for by baroclinic properties (i.e. conversion of potential into kinetic energy). There is, however, overwhelming evidence that the propagation of weather systems on the synoptic scale can largely be accounted for within a barotropic model and that at mid-tropospheric levels this model accounts for the major part of the observed changes. Consequently, in a dynamic approach to upper level prognosis it is logical to start with the barotropic solution. It is expected that a systematic study of the barotropic model, through its inadequacies, will indicate the nature and scale of baroclinic, terrain and other effects.

2. Fjörtoft (1) has provided a simple graphical method for obtaining the geostrophic vorticity and a similar technique for integrating the barotropic vorticity equation. At the Central Analysis Office the vorticity charts (2) have been used for several years in conjunction with Petterssen's (3) diagnostic equation for development to predict the location and timing of sea-level cyclogenesis. More recently experiments have been conducted on the complete graphical solution at 500 mb using a variation on the Fjörtoft technique. In view of the widespread use of barotropic models in objective prognosis the general model and the graphical type of solution are presented.

3. The basic equation governing synoptic scale motions in a barotropic atmosphere is:

3.1. $\frac{\partial \zeta}{\partial t} = \left(\frac{\partial v}{\partial x} - \frac{\partial u}{\partial y} \right)$ where ζ is the vertical component of relative vorticity; \vec{V} is the geostrophic wind and $f = 2\Omega \sin \phi$, the coriolis parameter. The equation expresses the conservation of absolute vorticity ($\zeta + f$) on the assumption of horizontal, non-divergent motion at a level near 500 mb.

The geostrophic wind is given by:

3.2. $\vec{V} = \frac{g}{f} \mathbf{k} \times \nabla_s Z$ where \mathbf{k} is the unit vertical vector, $\nabla_s = i \frac{\partial}{\partial x} + j \frac{\partial}{\partial y}$ and Z is the height of a constant pressure surface. The geostrophic relative vorticity is given by

3.3. $\zeta = \frac{g}{f} \nabla_s^2 Z$ where ∇_s^2 is the surface spherical Laplacian operator. Now if we let the geostrophic absolute vorticity be (η) where

3.4. $\eta = \frac{g}{f} \nabla_s^2 Z + f$ the equation 3.1. may be written by substituting for \vec{V} and ζ as:

3.5. $\frac{\partial}{\partial t} (\nabla_s^2 Z) = -\mathbf{k} \times \nabla_s Z \cdot \nabla \eta = -\mathbf{k} \cdot \vec{v} \times \nabla \eta$ and by expanding the triple scalar product on the right side of 3.5.

$$3.6. \quad \frac{\partial}{\partial t} (\nabla_s^2 Z) = \frac{\partial \eta}{\partial x} \frac{\partial Z}{\partial y} - \frac{\partial \eta}{\partial y} \frac{\partial Z}{\partial x}$$

where the right side of 3.6 is equal to $J(\eta, Z)$, the well known Jacobian determinant of η and Z with respect to X and Y . Then interchanging the order of differentiation on the left side of 3.6, the equation becomes:

$$3.7. \quad \nabla^2 \left(\frac{\partial Z}{\partial t} \right) = J(\eta, Z)$$

The Jacobian ($J(\eta, Z)$) is thus a representation of the advection of absolute vorticity (η) in the constant pressure (Z) field. Equation 3.7. is the basic equation in nearly all barotropic models adapted for numerical computations and forms a part of most models (4).

This is a Poisson equation where $\left(\frac{\partial Z}{\partial t} \right)$ is the unknown; $J(\eta, Z)$ involves only local space derivatives of η and Z (equation 3.6.) and can be computed from a constant pressure chart. The solution of this equation varies with the method; in machine techniques the solution is usually achieved by relaxation (successive approximation) techniques. The solution given here is adaptable to graphical hand techniques.

4. The spherical earth is mapped conformally onto a plane. If "m" is the magnification factor in the transformation from spherical coordinates to the particular map projection used in the computations, the Laplacian and Jacobian operators transform as follows:

$$4.1. \quad \nabla_s^2 = m^2 \nabla^2 \quad ; \quad J_s = m^2 J$$

and 3.7. is thus transformed to:

$$4.2. \quad \nabla^2 \left(\frac{\partial Z}{\partial t} \right) = J(\eta^*, Z)$$

where ∇^2 and J are plane operators and

$$4.3. \quad \eta^* = \frac{g}{f} m^2 \nabla^2 Z + f$$

The geostrophic vorticity in (4.3.) is obtained, after Fjörtoft (1), by substituting the finite difference approximation for $\nabla^2 Z$ as given by:

$$4.4. \quad \nabla^2 Z = -\frac{1}{d^2} (\bar{\bar{Z}} - Z)$$

where d is the grid length and the bar ($\bar{\bar{\quad}}$) operation is defined by:

$$4.5. \quad \bar{\bar{Z}} = \frac{1}{4} [Z(x+d, y) + Z(x-d, y) + Z(x, y+d) + Z(x, y-d)]$$

Thus equation 4.2. becomes

$$4.6. \quad -\frac{A}{f^2} \frac{\partial}{\partial t} (Z - \bar{\bar{Z}}) = J \left[\left(-\frac{4gm^2}{f^2} (Z - \bar{\bar{Z}}) + f \right), Z \right] \\ = -k \cdot \nabla Z \times \nabla \left[\left(-\frac{4gm^2}{f^2} (Z - \bar{\bar{Z}}) + f \right) \right]$$

Consider the extreme right term of the triple scalar product (4.6.) then:

$$4.7. \quad \nabla \left[-\frac{4gm^2}{f^2} (Z - \bar{\bar{Z}}) \right] \cdot \nabla Z = -\frac{4gm^2}{f^2} \left[\nabla (Z - \bar{\bar{Z}}) - \frac{1}{f} \nabla f \right] \cdot \nabla Z$$

on the assumption that $\nabla \frac{1}{f} \ll \nabla (Z - \bar{\bar{Z}})$ and since the last term on the right in (4.7.) varies only with latitude it can be replaced by the gradient of $G(\phi)$ where

$$4.8. \quad G(\phi) = \int \frac{d^2 f}{4gm^2} \cot \phi \, d\phi$$

substituting back into 4.6. we obtain

4.9.
$$\frac{\partial}{\partial t} (z - \bar{z}) = \frac{gm^2}{f} J(z - \bar{z} - G(\phi), z)$$

This is essentially the model equation used by Fjörtoft (1). The function $G(\phi)$ represents an approximate contribution of the earth's rotation to the absolute vorticity. Since f and m are functions of latitude only, the value of $G(\phi)$ can be charted once and for all for a given map projection and grid distances.

The equation (4.9) represents the conservation of the quantity $(z - \bar{z} - G(\phi))$ and its advection in the 500 mb (z) field. Consequently, when the equation is solved to determine a height tendency $\left(\frac{\partial z}{\partial t}\right)$ the finite time interval (Δt) over which this tendency can be applied depends largely on the variations in time of the advective field. An ingenious method for increasing the time interval (Δt) to the order of 24-36 hours has been developed by Fjörtoft (1) whereby the advection field (z) is replaced by the less varying field of \bar{z} (space mean).

The principle underlying the replacement of the z -field by the \bar{z} -field can be shown as follows: if α and β are two scalar fields then from the definition of determinants we have

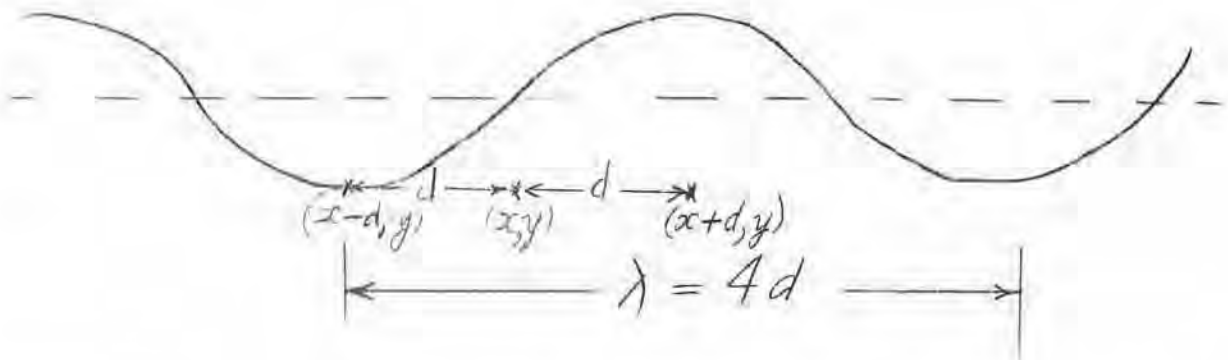
4.10.
$$J(\alpha, \beta) = J(\alpha, \beta - \alpha)$$

Substituting this result in 4.9. then

4.11.
$$\frac{\partial}{\partial t} (z - \bar{z}) = \frac{gm^2}{f} J(z - \bar{z} - G(\phi), \bar{z} + G(\phi))$$

which expresses the conservation of the $(z - \bar{z} - G(\phi))$ field in the advective $(\bar{z} + G(\phi))$ field.

5. Fjörtoft (1) deals further with the nature of the finite difference approximation given by equation 4.4. It is clear that by definition the \bar{z} -field is a space average of the z -field and that $(z - \bar{z})$ -field is a representation of the vorticity field. By utilising Fourier coefficients Fjörtoft goes on to show that the space mean process is most effective when the wave length (λ) of the disturbance is equal to four times the grid distance (i.e. $\lambda = 4d$)



It is clear from the above diagram that in the case of a simple sine wave when $\lambda = 4d$ then the point $(x + d, y)$ is on the ridge line and the point $(x - d, y)$ is on the trough so that adding over the complete wave range results in a straight line space mean (\bar{z}); hence the smoothing is complete

and the wave does not appear in the space mean. It is also clear that when $d = 0$ that $\bar{z} = z$ and there is no solution. The Fjörtoft choice of a grid distance of 360 N.M. (12° Long) at 60°N is thus most effective in smoothing out, or filtering for wave lengths on the scale equivalent to 48° Long at 60°N . The work at the Central Analysis Office (1) confirms the usefulness of this grid distance for the 500 mb short waves associated with moving disturbances. It was also shown that the most effective empirical relationship for advection was to use 80% of the \bar{z} -field and that for this grid distance (360 N.M.) the $G(\phi)$ term was small enough to be neglected.

6. Up to this stage we have been concerned with the evaluation of the right hand of the model equation. In order to obtain a complete solution it is necessary to solve the Poisson equation $\nabla^2(\frac{\partial z}{\partial t}) = J(\dots)$, or its finite difference form $\frac{\partial}{\partial t}(z - \bar{z}) = J$. Following a similar treatment to Fjörtoft (1) this can be achieved as follows.

One can write the following identity:

$$6.1 \quad \Delta z \equiv \Delta z - \Delta \bar{z} + \Delta \bar{z} - \Delta \bar{\bar{z}} + \Delta \bar{\bar{z}} - \Delta \bar{\bar{\bar{z}}} + \Delta \bar{\bar{\bar{z}}} - \dots - \Delta \bar{\bar{\bar{\bar{z}}}} + R_L$$

where Δ represents finite time difference; the bar ($\bar{\quad}$) operation is a space average as defined in (4.5.), and successive space averages are taken up to the number L and $\Delta \bar{\bar{\bar{\bar{z}}}} = R_L$ the remainder (Note that in right side of 6.1. every other term cancels the previous one). Now this can be grouped as

$$6.2 \quad \Delta z \equiv \Delta(z - \bar{z}) + \Delta(\bar{z} - \bar{\bar{z}}) + \dots + \Delta(\bar{\bar{\bar{\bar{z}}}} - \bar{\bar{\bar{\bar{\bar{z}}}}}) + R_L$$

Then by substituting

$$6.3 \quad \xi^k = z - \bar{z}, \quad \xi^{k'} = \bar{z} - \bar{\bar{z}}, \quad \xi^{k''} = \bar{\bar{z}} - \bar{\bar{\bar{z}}}, \text{ etc.}$$

One obtains for 6.2. that

$$6.4 \quad \Delta z = \Delta \xi^k + \Delta \xi^{k'} + \Delta \xi^{k''} + \dots$$

Then by substituting values for the finite time difference

$$6.5 \quad z_t - z_0 = \xi_t^k - \xi_0^k + \xi_t^{k'} - \xi_0^{k'} + \dots \\ = \xi_t^k - (z_0 - \bar{z}_0) + \xi_t^{k'} - (\bar{z}_0 - \bar{\bar{z}}_0) - \dots$$

and grouping terms.

$$6.6 \quad z_t = \bar{z}_0 + \xi_t^k + \xi_t^{k'} \quad \text{or} \quad = \bar{z}_t + \xi_t^k$$

providing that the series converges fast enough i.e., that the double space mean chart does not change significantly with time (ie $\Delta \bar{\bar{z}} \approx 0$). Fjörtoft shows that this type of series converges rapidly with the proper choice of grid distances. In our solutions the grid distances are chosen as follows:

$$\bar{z}, d_1 = 12^\circ \text{ long at } 60^\circ\text{N}; \quad \bar{\bar{z}}, d_2 = 24^\circ \text{ long at } 60^\circ\text{N} \\ \bar{\bar{\bar{z}}}, d_3 = 48^\circ \text{ long at } 60^\circ\text{N}$$

It is thus clear that the \bar{Z} operation filters disturbances with wave lengths of the order of 48° long at 60°N ($4d$); the \bar{Z} operation filters wave lengths of the order of 96° long at 60°N and the \bar{Z} would filter at 192° long. In practice then it appears sufficient to carry the solution only to the \bar{Z} stage as indicated in (6.6.).

In equation 6.6. then Z_t is the forecast 500 mb chart, \bar{Z}_0 is the double space mean chart; ξ_t is the forecast (short wave) vorticity field ($Z - \bar{Z}$) and ξ'_t is the forecast (long wave) vorticity field ($\bar{Z} - \bar{Z}$).

It was indicated earlier that the $G(\phi)$ term could be neglected for a grid distance of 360 N.M. This term (4.8.) varies with the square of the grid distance and cannot be neglected at $d_2 = 720$ N.M. $G(\phi)$ is equivalent to an east wind having magnitudes at 45°N of ≈ 4 kts for $d_1 = 360$ N.M. and 16 kts for $d_2 = 720$ N.M. The operating procedures for obtaining the 500 mb prog as given by 6.6. are outlined in Appendix B.

In practice, as would be expected, the \bar{Z} - chart varies little, the \bar{Z} - chart varies appreciably and the Z - chart varies most rapidly. It is thus an advantage to carry out the advection of the large scale vorticity field ($\bar{Z} - \bar{Z}$) and by adding this to the \bar{Z}_0 - chart obtain the \bar{Z}_t - forecast space mean chart. Hence one can obtain a forecast space mean chart for the mid or end point of the prog period and thus modify the advective \bar{Z} field for moving the most rapidly changing (ξ) components of the velocity field. It is also evident that in the form (6.6.) the forecast time can be varied across the chart and a composite prog obtained.

7. The major part of the work, i.e. graphical addition and subtraction, could be carried out by training technical personnel with the meteorologist required only for the advection portion. The success of the experimental prognostics to date gives the optimistic hope that the technique can provide a sound objective basis for the upper level progs. Most tests have however been during the summer season when barotropic approximations are more valid. In the minimum the charts provide the basis for a better dynamic understanding of atmosphere process and a sound introduction to numerical techniques. It is expected that these progs will be treated as the objective basis on which to build baroclinic dressing and not as simply an additional background forecast tool.

The next step is to attempt as in (5) to extend this technique to more than one level (to obtain surface progs) and to include baroclinic effects.

8. Example

Fig. 1 shows the 500 mb (Z) chart for 0300Z 11 June 56 together with the space mean (\bar{Z}) chart and the vorticity field ($Z - \bar{Z}$) field. Three significant short wave troughs appear over the continental area; these are clearly depicted by the cyclonic vorticity centers of -350 ft near Seattle, Wash., -400 ft near Coral Harbour, NWT. and -300 ft south-east of Montreal. A weaker center is

also present near Rapid City, S. D. The space mean (\bar{Z}) chart is relatively smooth in comparison to the 500 mb chart but still shows clearly two large scale troughs, one near 132W off the West Coast and one near 67W in the eastern section.

Fig. 2 shows the double space mean ($\bar{\bar{Z}}$) chart, the large scale vorticity field ($\bar{Z} - \bar{Z}$) and the advective field ($\bar{Z} + G(\phi)$). The double smoothing has washed out the two large scale troughs of the \bar{Z} -chart. In this case the two troughs were spaced at a distance equal to $4d_2$ ($d_2 = 720$ N.M. at 60°N); the distance at which the space smoothing is most effective. It can readily be seen that the correction required when averaging over such a large latitudinal interval (24 deg.) is appreciable; the ($\bar{Z} + G(\phi)$)-chart shows that over most of the mid-latitude regions the westerly component of the \bar{Z} -field has been completely compensated by the easterly component of the $G(\phi)$ -field resulting in very little motion for the large scale waves.

Fig. 3 shows the 500 mb prog and the verifying chart. The vorticity lines ($\bar{Z} - \bar{Z}$) were advected with 80 percent of the \bar{Z} -field and the large scale ($\bar{Z} - \bar{Z}$) lines with the full geostrophic ($\bar{Z} + G(\phi)$)-field. The two sets of forecast vorticity lines ($\bar{Z} - \bar{Z}$)₃₆ and ($\bar{Z} - \bar{Z}$)₃₆ were added to the \bar{Z}_0 -chart to give the forecast 500 mb chart.

It can be seen that the prog chart, on the whole, worked out very well.

The low south of Great Slave Lake is very close in position but the actual is 300 ft deeper. Even though baroclinic development has taken place the position and structure of this system verifies very well.

The system near Cap Chidley also verifies well as to position but the actual trough has intensified southeastward more rapidly. As a consequence the forecast wind pattern is still good on the west side of the trough but has become poor on the east side. The cutting off and general position of the low south of Nova Scotia has been forecast well but the same type of error in gradients again appears. It is clear that these eastern systems are still quite good representations of the actual at time $t = 36$ hrs, but the degree of representation would decrease rapidly beyond this time. The tendency for the method to advect the vorticity around large scale troughs too rapidly has been noted previously (1) and appears to be an inherent error of the method.

The prog chart scored very well. The objective gradient score (6), where $s = 100 e_G/G_L$ was

$$s = 51.0$$

The correlation coefficient between the forecast and observed heights over the same grid points as used for s was:

$$r = 0.86$$

with a root mean square error:

$$\text{RMSE} = 166 \text{ ft.}$$

REFERENCES

1. Fjörtoft, R., 1952: On a numerical method of integrating the barotropic vorticity equation. *Tellus*, 4, 179-194.
2. Kwizak, M., 1956: Vorticity and cyclogenesis. TEC - (to be published).
3. Petterssen, S., 1955: A general survey of factors influencing development at sea-level. *J. Meteor.*, 12, 36-42.
4. Thompson, F. D. and Gates, Lawrence W., 1956: A test of numerical prediction methods based on the barotropic and two-parameter baroclinic models. *J. Meteor.*, 13, 127-141.
5. Estoque, M. A., 1956: A prediction model for cyclone development integrated by Fjörtoft's method. *J. Meteor.*, 13, 195-202.
6. Boville, B. W., 1956: Verification of prognostic charts issued by the Central Analysis Office. TEC - (to be published).

Appendix ASpace Means by Graphical Techniques

1. Since the geostrophic vorticity is defined by $\zeta = \frac{g}{f} \nabla^2 Z$ a solution can be obtained by using the finite difference approximation for the Laplacian ($\nabla^2 Z$) i.e. $\nabla^2 Z = -\frac{g}{f d^2} (Z - \bar{Z})$

The bar operator ($\bar{\quad}$) defines a space average over the grid distance, d , such that $\bar{Z}(x, y) = \frac{1}{4} (Z(x+d, y) + Z(x-d, y) + Z(x, y+d) + Z(x, y-d))$. This space meaning of a scalar field can be carried out at discrete points as in diagram 1 or for a complete chart by graphical addition.

$$\begin{array}{c} \times Z(x, y+d) \\ | \\ Z(x-d, y) \times \text{---} \times Z(x, y) \quad Z(x+d, y) \\ | \\ \times Z(x, y-d) \end{array}$$

2. For graphical addition two copies, A and B, of the 500 mb chart (e.g. a transparency and one ozalid copy) are required.

The charts A and B are separated vertically (along the y - axis) a distance equal to $2d$, and then added graphically onto a blank chart C, centered between A and B. (In the solution for \bar{Z} , $d = 360$ N.M. and the two charts are separated a distance equivalent to 12 deg. of Lat. at 60°N). During the addition every other contour is dropped and the chart, C, thus provides a solution over the entire chart for $\frac{1}{2} (Z(x, y+d) + Z(x, y-d))$

In a similar fashion the two charts are separated horizontally and added onto a centered chart, C_1 , to obtain the solution along the x - axis.

Adding charts C and C_1 , again dropping every other contour, then gives a complete chart of the contours of \bar{Z} . Due to the nature of the averaging process sections of width, d , are lost on all four sides from the area covered by the original (Z) chart.

The $(Z - \bar{Z})$ chart can readily be obtained by graphical subtraction of the 500 mb and space mean charts.

Appendix BGraphical Barotropic Prog Procedures

1. Analysis Steps:
 - 1.1. With a grid distance, $d_g = 360$ N.M. at 60°N , and the the 500 mb (Z) chart apply the space mean procedures of Appendix A to obtain the charts: \bar{Z}_0 and $(Z - \bar{Z})_0$.
 - 1.2. With a grid distance, $d_g = 720$ N.M. at 60°N , repeat the space mean operation on the \bar{Z}_0 chart (instead of the Z - chart) to obtain: \bar{Z}_0 ; $(\bar{Z} - \bar{Z})_0$ and $(\bar{Z} + G(\mathcal{G}))_0$.

2. Prog Steps:
 - 2.1. Advect the $(\bar{Z} - \bar{Z})_0$ isolines in the $(\bar{Z} + G(\mathcal{G}))_0$ field at the full geostrophic speed given by the field to obtain $(\bar{Z} - \bar{Z})_t$.
 - 2.2. Add \bar{Z}_0 and $(\bar{Z} - \bar{Z})_t$ to obtain \bar{Z}_t .
 - 2.3. Advect the $(Z - \bar{Z})_0$ isolines in the \bar{Z} field using 80% of the geostrophic speed given by the field to obtain $(Z - \bar{Z})_t$.
 - 2.4. Add \bar{Z}_t , from 2.2. and $(Z - \bar{Z})_t$, from 2.3. to obtain the prog 500 mb chart, Z_t .

Values of Function $G(\phi)$

The values of $G(\phi)$, in units of feet, are tabulated below at intervals of 5 degrees latitude and for $d = 360$ N.M. and $d = 720$ N.M. for a conformal conic map with standard latitudes at 30 and 60 degrees.

LAT.	90	85	80	75	70	65	60	55
$G(\phi)$ for $d = 360$ N.M.	376	375	370	359	344	323	296	263
$G(\phi)$ for $d = 720$ N.M.	1504	1500	1480	1436	1376	1292	1184	1052

LAT.	50	45	40	35	30	25	20
$G(\phi)$ for $d = 360$ N.M.	227	191	155	119	88	60	38
$G(\phi)$ for $d = 720$ N.M.	908	764	620	476	352	240	152

(blank page)

500 mb, 0300Z, JUNE 11, 1956

Legend
— (Z), 500mb
- - - (Z̄), Space Mean
= = = (Z - Z̄), Vorticity
units, hundreds of feet

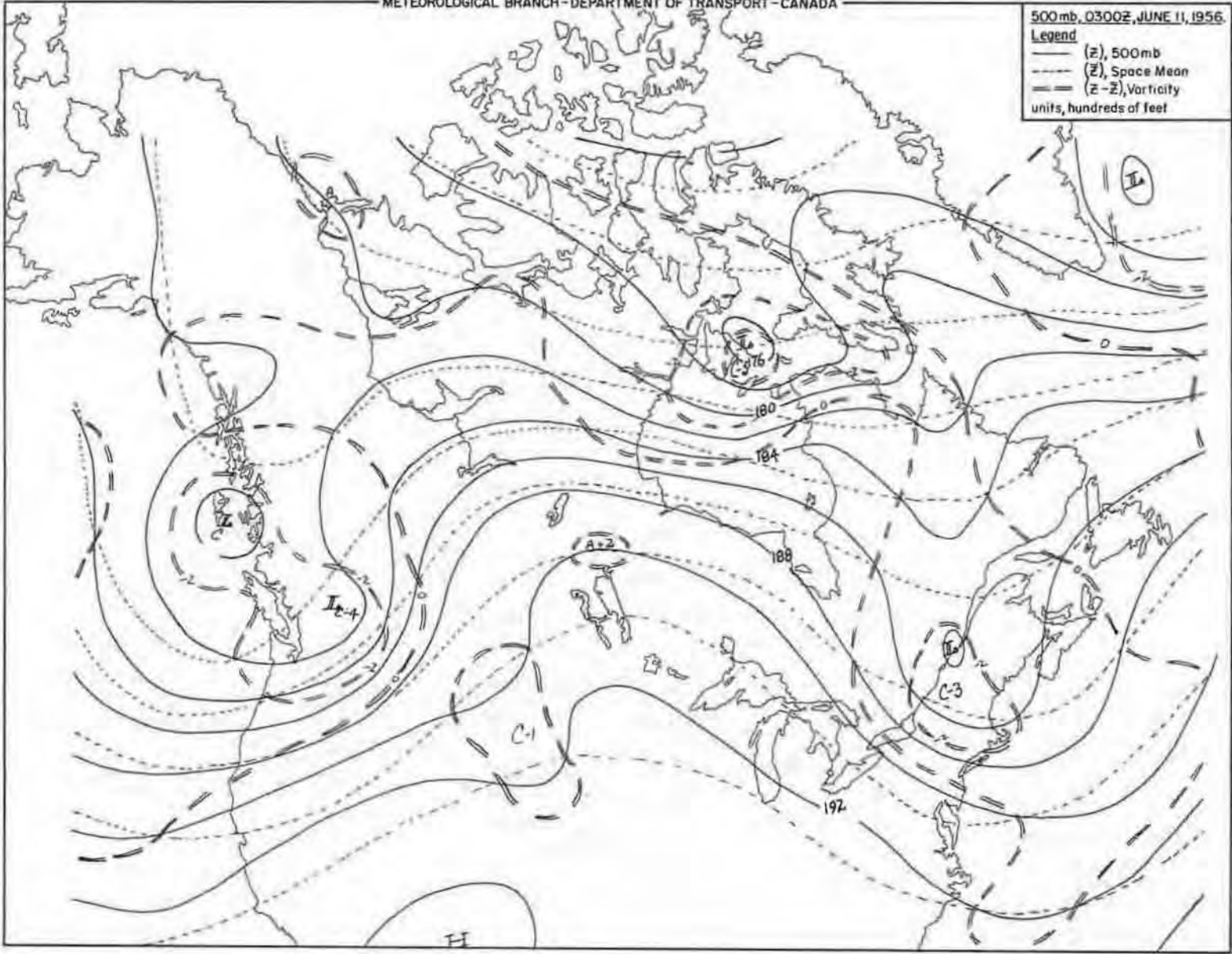


FIGURE 1

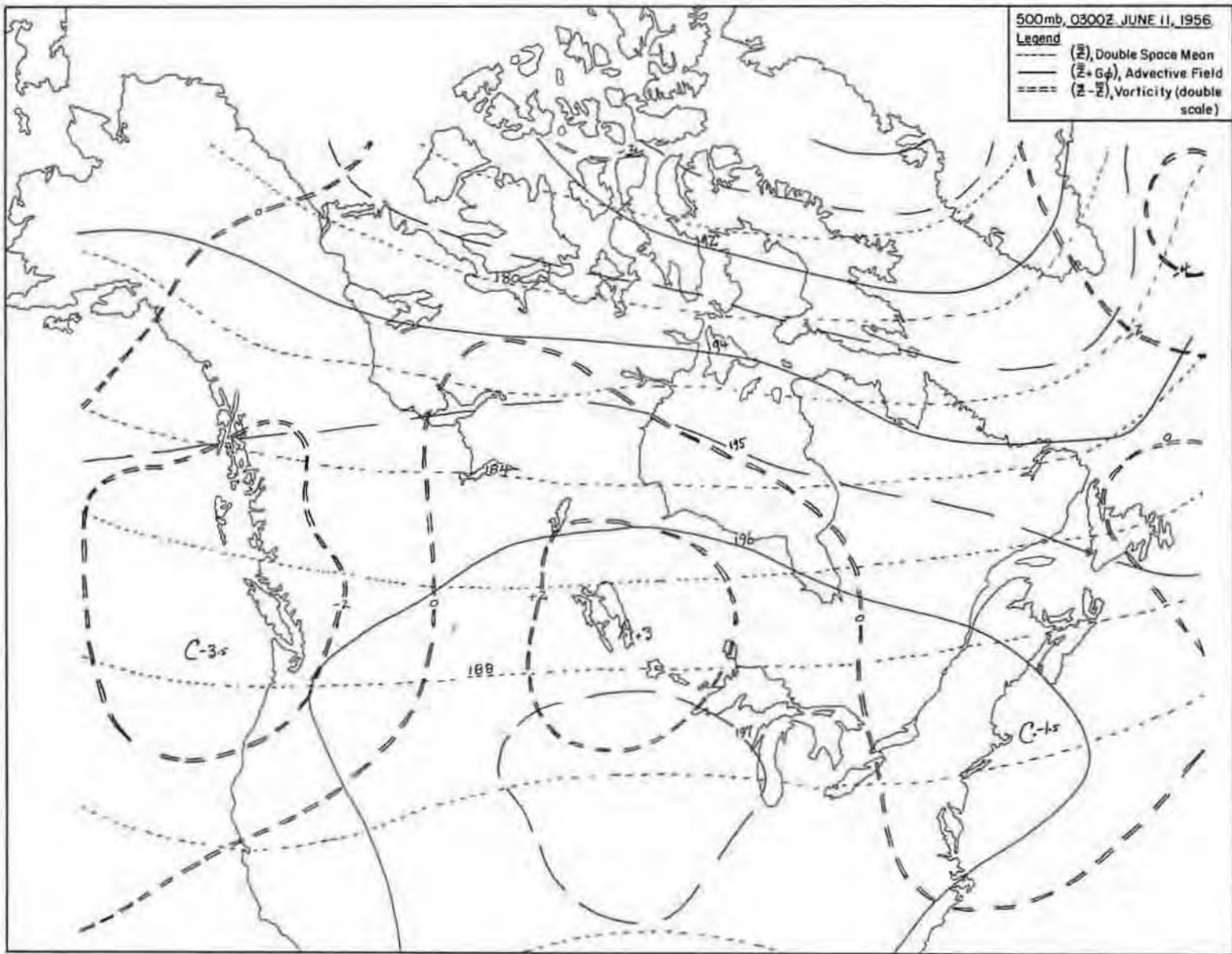


FIGURE 2

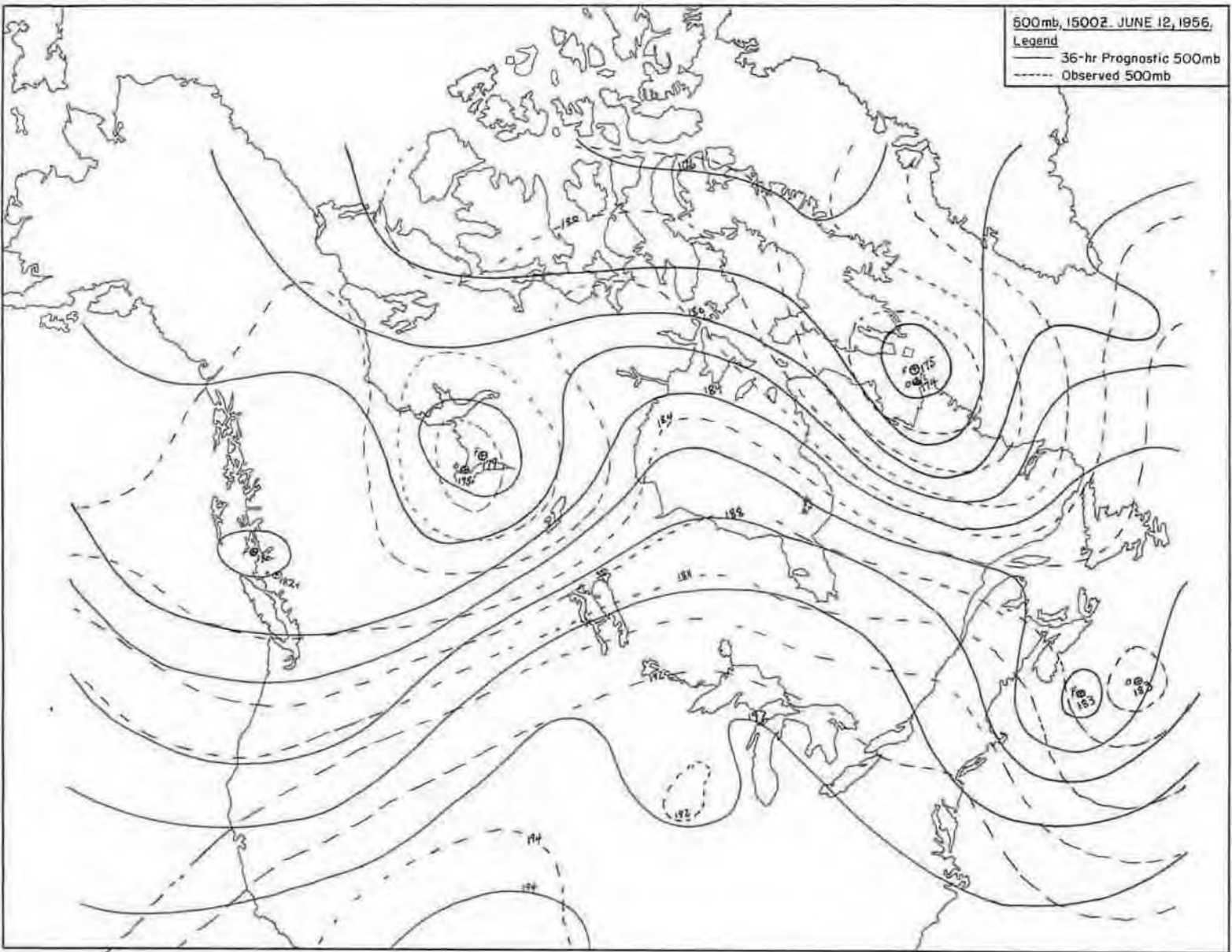


FIGURE 3

(blank page)

PRELIMINARY REPORT ON OZONE CHANGES 1950-1954 OVER EDMONTON

by E. H. Gowan, S. J. Buckler, C. E. Thompson

A B S T R A C T

The ozone measurements over Edmonton have been analyzed to find relationships between changes of ozone amount and weather map features at the 500-mb level. To date the five years of ozone observations from Edmonton are the only Canadian measurements of ozone. This study is a pilot project to suggest methods of using the increased ozone measurements to be obtained during the International Geophysical Year.

At high levels there is a fairly good negative correlation between ozone amount and the height of a given pressure surface. Particular attention has been given to short wave troughs of 2-3 day periods at the 500-mb level. For many cases the ozone increases as the trough moves over the station. This is shown by values (dated) on maps for the 500-mb surface, and also by graphs showing ozone changes for days before and after the trough passage.

It seems evident in most cases that both subsidence and advection are important in ozone changes. Over 500-mb troughs subsidence appears to be most important. To the west of these troughs horizontal advection is the important factor.

INTRODUCTION

Measurements of Atmospheric Ozone have been made at Edmonton since August 2, 1950, using the Dobson Ozone Spectrophotometer belonging to the Meteorological Service of Canada. Daily values of ozone have been tabulated. Ten-day mean values have been calculated for the three 10-day periods each month, and a table of smoothed 10-day means constructed for the period 1950-54. Previous investigators using part of these data, by Gowan and Leppard (1953) and Dennis (1954), studied some of the relationships between ozone changes and meteorological factors.

SEASONAL RELATIONSHIPS

The 10-day averages, Fig. 1, show a pronounced seasonal maximum in March followed by a seasonal minimum in October. Both the seasons of maximum and minimum, and the magnitude of the ozone values, agree very well with Dobson's published results for Oxford, England, at a latitude of 51°N (cf Edmonton 53°N). Also shown on the Edmonton curve is a secondary maximum in early December. This secondary maximum also occurs in the curve for Bismarck, North Dakota, (2 years 1953-54). Both Bismarck and Edmonton are well inland and the secondary maximum may be a continentality factor of the North American stations.

An attempt was made to find a relationship between ozone values at Edmonton and later at Bismarck, to indicate transport of ozone. No conclusive results were noted by inspection, and it is suggested that this be pursued, using the new U. S. series of 50 and 25 mb charts for trajectory studies.

UPPER ATMOSPHERE RELATIONSHIPS

Craig (1950) discusses the relation between photochemical computations of total ozone amounts and the observed values. He points out that there must be atmospheric processes which transport ozone from high levels (where it will be replaced by new ozone formed by photochemical action), to lower levels where the ozone is protected from photochemical action. Umkehr and other measurements show that the large daily changes in ozone occur in the interval from 10 to 20 kms. Fig. 2 shows the ozone distribution at Edmonton on Sept. 8, 1953, calculation made by the Umkehr method. The authors felt that an examination of upper air charts might show this process or at least point toward it.

Dennis (1954) compared the variation of mandatory levels above 500 mb and the tropopause, with daily mean ozone values for the year 1953, and found a negative correlation. The correlation appeared to be equally good for all levels. (See table 1). He also examined eighteen 500-mb troughs but could draw no conclusion relating the ozone values to the 500-mb troughs.

Normand (1953) studied long wave fluctuations (5-14 days), and found a close relationship between ozone changes, the height of the tropopause, and the 300-500 mb thickness. He later reported (1954) that on the basis of three years' observations the best correlation was with the 300-mb

height. He also reported that similar correlations existed with some short wave changes with a period of approximately two days. However no systematic examination was made of these shorter periods, partly because of the difficulty that ozone observations did not coincide well enough with the short period systems.

The following work was designed to study the ozone relation between these short waves of two to four-day periods, using the ozone observations at Edmonton for the available years 1950-55, and the 500-mb charts for the same period. The latter charts were chosen for the reason that they are the highest regularly analyzed charts readily available for the interval, and because the authors have been accustomed to following short waves in the 500-mb analysis; and further, Dennis' table showed no significant loss by using 500-in preference to 300- or 200-mb level.

FURTHER STUDY OF THE 500-MB SURFACE AND OZONE VARIATIONS

To examine a trough the following procedure was used: first a series of 500-mb maps was examined for a period of two to four days while a trough moved past Edmonton; by inspection a best fit was selected from the series, usually the one where Edmonton was nearest the trough line - this was traced with wax pencil on an acetate transparency and the Edmonton position indicated. The transparency was then laid over other maps in the series making the trough line and one contour coincide. Sometimes adjustment was necessary as a trough developed a closed contour, or deepened or filled markedly. Since the Edmonton ozone observations were generally taken at 1800Z or 2100Z, the 1500Z charts were selected as being nearest the time of ozone reading.

The case was then transferred to paper over a light table, and the ozone data were plotted in the appropriate position. The plotting model contained the actual ozone amount, normal value from the smoothed curve of ten-day means, ozone change in the previous 24 hours (ozone tendency), and deviation of actual value from the mean (anomaly); e. g.,

August 26	231	-27
	236	- 5

231 means that the total thickness of ozone over Edmonton was .231 cms at NTP.

These charts of single tracks were then assembled in composite charts, grouping December, January and February; March, April and May; June, July and August; and September, October and November, for each year. This was done by selecting a best fit for the season and using it as a master chart. Others in the same season were transferred to the best fit, by making trough line and one selected contour fit as closely as possible. In nearly every season it was possible to portray a season's result on one chart.

Cold lows were treated separately, but in a similar manner. When assembling a composite chart for a season's cold lows, the center and one open contour were made to coincide. Distinction was made between two types of cold lows, the Alberta Summer Type, and the Hudson Bay Cold Low in which a trough swings around the low center, passing over Edmonton.

RESULTS

To date, the upper air maps for three of the five years for which ozone values are available, have been examined and composite charts prepared. Figures 3 to 12 show seasonal charts.

As might be expected, the Spring chart (Fig. 8) (for period of maximum ozone content in the atmosphere), shows the greatest day to day variations in ozone, amounts ranging from .035 cm to .099 cm. The Fall chart (for season of minimum ozone content), shows smaller day to day variations.

Isallopleths of 24-hour ozone change, or ozone tendency, have been drawn on these charts. A rather uniform picture was portrayed on all but the Summer charts. About 750 miles east of the trough line a small negative tendency usually occurs. This quickly changes to a positive tendency.

The increase in ozone becomes very marked, reaching a maximum sometimes before and sometimes after the trough line, to be followed by a strong negative tendency field west of the trough. The net effect is to show the positive tendency field as an elongated or double maximum field, and the negative area as a more sharply defined system.

Reed (1950) has shown that in temperate latitudes a maximum of .040 cms variation can properly be credited to vertical motion, and that approximately .080 cms is the maximum change derived from advection. It is on the west side of the trough that horizontal transport will cause an increase in ozone, by reason of the normal northward increase in ozone values except in Autumn. This explains the increases found occasionally to the rear of the trough lines and some of the greatest increases found there. The centers of ozone increase in or east of the trough would appear to be the result of subsidence.

With the short period waves that we are studying here, the ozone negative tendency is found on the ridge following the trough. In other words we have come to the opposite process whereby air of low ozone content has been transported northward to a region where the ozone content is normally higher. Similarly the air has been subject to lift which again decreases the total ozone.

The small negative values well in advance of the trough, which appeared in Fig. 7 and 8, were due to the fact that at this distance east of the trough we are on the next ridge downstream, and so are seeing the same phenomenon that is found on the ridge upstream from the trough.

ANOMALIES

Another valuable method of examining the trough-ozone relationship is to draw the isopleths of ozone anomaly (difference between the ozone amount for any day and the normal for that day). The value for these anomalies has been plotted in Figs. 3 - 12 but for clarity Figs. 13 - 16 have been prepared showing the isopleths of anomaly. In general these isopleths have a relatively simple pattern. Fig 15 is a good example of the simplest pattern. The positive anomaly center lies in the trough, with negative anomalies east and west of the trough. The positive anomaly center may not be symmetrically located with respect to the trough but certainly is definitely connected with it. An

example of a more complex pattern is shown in Fig. 16. Although the studies were of short wave troughs, some of these may be involved with the long wave pattern. Fig. 16 has a large area of positive anomaly east of the trough and west of the trough with only a small area of negative anomalies west of the trough. A long wave trough east of the short wave trough would account for the rises.

Epstein and others (1956), have shown graphically how ozone over Arizona varies with the passage of eight troughs on the 500-mb surface. They found maximum increases in ozone occurring from two days before trough passage to two days after passage. Similar graphs have been constructed for the cases studied in 1952-53-54. Fig. 17 shows the graphic picture of ozone change by season for the year 1953. Epstein and his colleagues found changes of the order of .02-.05 cms, whereas the Edmonton changes ranged up to .099 cms. This graph shows the maximum positive tendency occurring within 24 hours of the trough passage, and illustrates in time the phenomena that have been described in space by the figures showing the contours and ozone tendency isograms. The time variation could also be shown by using the ozone anomalies at integral day values.

Many avenues of investigation are left open. All the tendencies for the period studied have been combined in Fig. 18. The same could be done for anomalies. These might be fitted by least squares to a polynomial (second order for tendencies or third order for anomalies). The study could be extended profitably to short wave ridges, and to long wave troughs and ridges. The assumptions that subsidence and advection in the ozone-rich layers are correlated with the upper flow patterns could also be examined by a study of the new U. S. series of 50 mb and 25 mb charts.

VARIATIONS IN THE TOTAL OZONE ASSOCIATED WITH THE HUDSON BAY COLD LOWS

The low at 500 mb in this case is found predominantly northeast of Edmonton with its mean position northwest of Hudson Bay. There were four cases of this in 1952-53. Using the March 2/52 500 -mb chart as a base, the other cases were fitted on it. The composite chart in Fig. 19 shows very high ozone values compared to normal. The isopleths of anomaly are drawn on this figure. Most of the extreme ozone values appear in these situations. Values approach normal or are below normal only in the July 3/53 case (preceding the passage of a trough June 30/53 extending from the cold low), and the Nov. 20/52 case. The extreme deviation from the mean occurred on July 4/53 when a positive .071 cm deviation occurred (27% above normal). Within a radius of 1200 miles from the center of the low the average deviation from the mean ozone values was .030 cm which is about 10% above normal. The highest ozone values are from 300 to 700 miles southeast of the center. The anomaly pattern indicates a possible maximum of ozone in the center of low with the ridge of positive anomaly extending southwest.

The day to day changes in ozone (24 hour tendency) are on the average positive within 800 miles southwest of the low. Negative changes occur beyond that.

The high values of ozone occur in the strong northwest flow with cold temperatures at 500 mb. Minor troughs extending out from the Hudson Bay cold low swing southward around the main low in a counter-clockwise direction bringing in fresh surges of ozone. The high ozone can be attributed to both

vertical motion and horizontal advection. The cold temperatures at 500 mb imply a low tropopause and therefore subsidence in the ozone-rich layers above the tropopause. As Read has shown, this subsidence can result in an increase of up to .040 cm of ozone. Except in the autumn northerly flow brings air from the maximum ozone belt near 60N to the regions of lesser ozone farther south.

VARIATIONS OF TOTAL OZONE WITH THE COLD LOW - ALBERTA SUMMER TYPE

The Alberta Summer type cold low is the type that normally has one or two closed contours (200 ft), and one or two 5-degree Celsius isotherms at 500 mb, Thompson 1950. Weatherwise they produce a proportion of summer rain in Alberta. These cold lows, unlike the Hudson Bay type, are travellers. They move in through B. C. and out over Alberta. The cases studied in 1952-53, Fig. 19, do not show the high values of ozone as do the Hudson Bay cold lows. In fact, the average ozone value is low. Within 800 miles radius from the low, values of ozone were .007 below normal, or about 3% low. In general, though not in each case, the approach of the low gives falling ozone tendencies, with rising tendencies close to the low or immediately after the passage of the low. The low values associated with the cold lows probably arise from the fact that the core of activity is relatively small, hence advection cannot play a significant part. High values probably occur in a limited zone near the center - our values closest to the center, viz., case 4 and case 2, showed the highest values. There is a ridge of positive anomaly southeast and west-southwest from the low. These values could be due to subsidence associated with the low. A general rule can only be developed by getting more cases with the cold low passing over or very close to the ozone recording station.

CONCLUSIONS

1. The Edmonton, Alberta, and Oxford, England, ozone amounts agreed well in latitudinal sense or actual values, and in the seasonal variation.
2. In a single station analysis study of fifty-two 500 mb short wave troughs for the period 1952-54 passing Edmonton, the ozone tendency seems to be a valuable parameter. The maximum ozone tendencies occur close to the trough line indicating that subsidence is a large factor in the change. Further increases after a trough passage show that advection plays a part.
3. Extreme ozone values associated with a quasi-stationary Hudson Bay Cold Low are produced by advection from northerly latitudes and subsidence at high levels. The Alberta Summer type cold low is more transient and indicates a small zone of positive tendencies near the cold low. Advection and/or subsidence occur only over limited areas in this case.

ACKNOWLEDGMENTS

Grateful acknowledgment is made of the painstaking criticisms and suggestions made by Dr. W. L. Godson, which are embodied in this study.

REFERENCES

- CRAIG, R. A. 1950 The Observations and Photochemistry of Atmospheric Ozone and their Meteorological Significance. Meteorological Monographs Vol.1, No.2
- DENNIS, J. N. 1954 MSc Thesis, unpublished.
- EPSTEIN, E. S., OSTERBERG, C. & ADEL, A. 1956 A New Method for the Determination of the Vertical Distribution of Ozone from a Ground Station. J. Meteor., 13: 319-334.
- GOWAN, E. H. & LEPPARD, R. E. 1953 Can. Journal of Physics 31: 702-713
- NORMAND, C. W. B. 1953 Atmospheric Ozone and the Upper-Air Conditions. Quart. J. R. Met., 79, p.39.
- 1954 Ozone and the Upper Atmosphere. Proceedings Toronto Met. Conference, p.6.
- REED, Richard J. 1950 The Role of Vertical Motions in Ozone-Weather Relationships. J. Meteor., 7: 263-267.
- THOMPSON, C. E. 1950 Cold Lows Affecting Alberta in Summer, (June - September). Dept. of Transport, Meteorological Branch, Technical Circular CIR-1813, TEC-76.

(blank page)

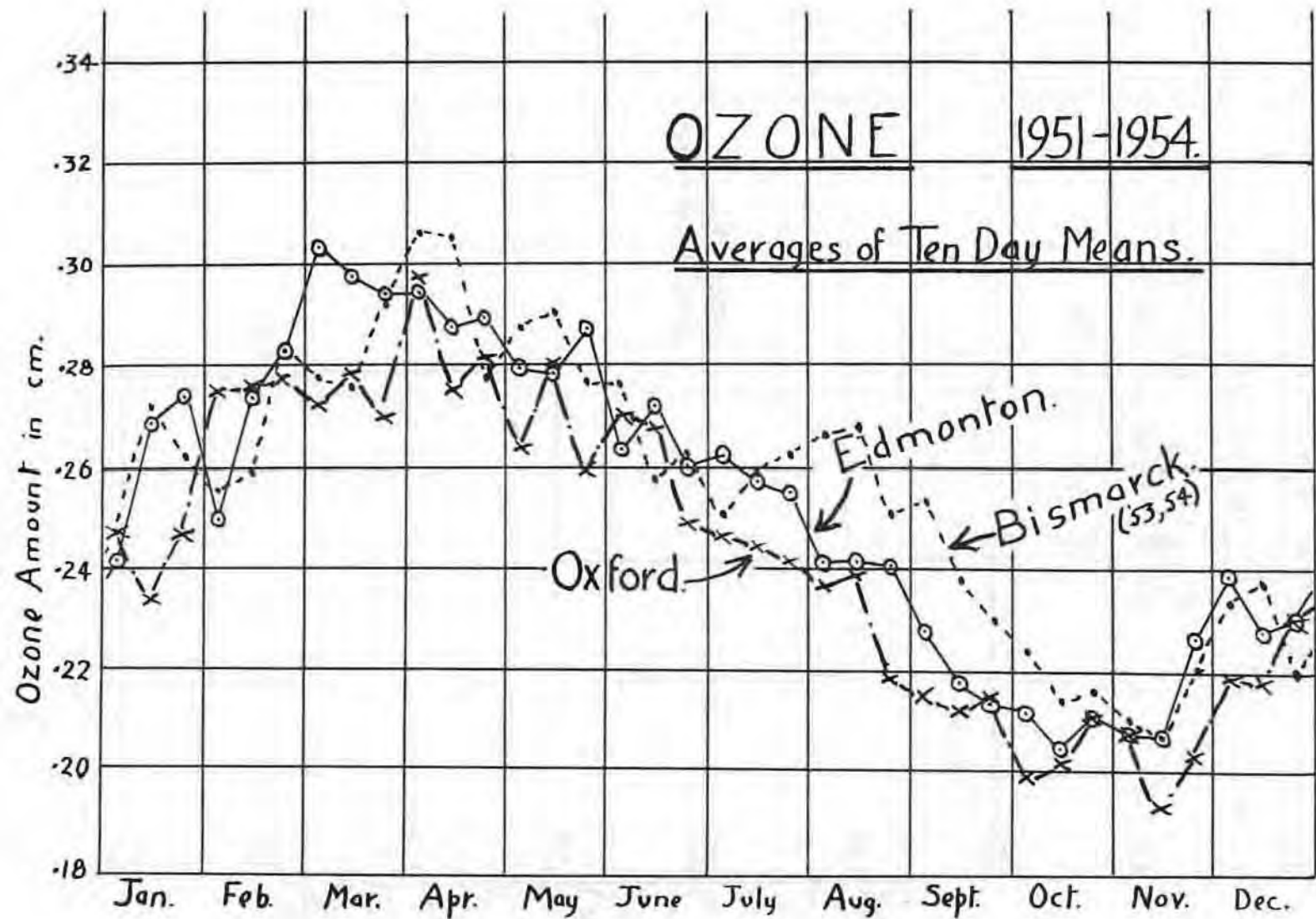


FIGURE 1

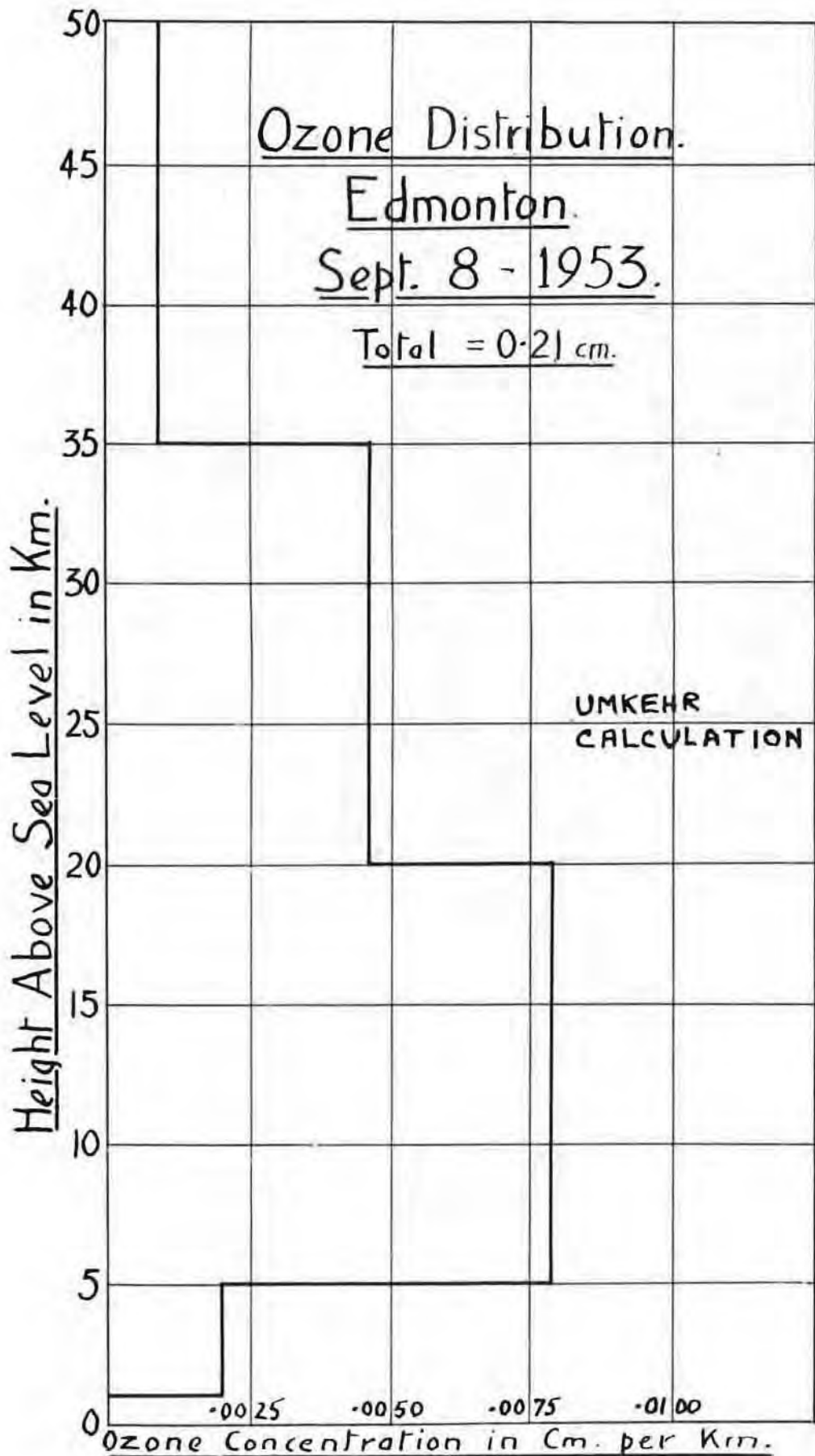


FIGURE 2

COMPOSITE OZONE	REFERENCE POINT	PLOTTING MODEL
Dec '51 - Feb 1952	USE JAN 4/52 15 ±	JAN 31/52
CASES of TROUGHS	25 BASE (500 MB)	SURRENT OZONE 283 +45 24HR TENDENCY
JAN 4/52 15 ±	ORIENT TROUGH	NORMAL OZONE 264 +19 ANOMALY
JAN 31/52 15 ±	AND INTERSECTION	
Feb 13/1952 15 ±	TROUGH LINE AND	
Feb 21/52 15 ±	17400 CONTOUR	

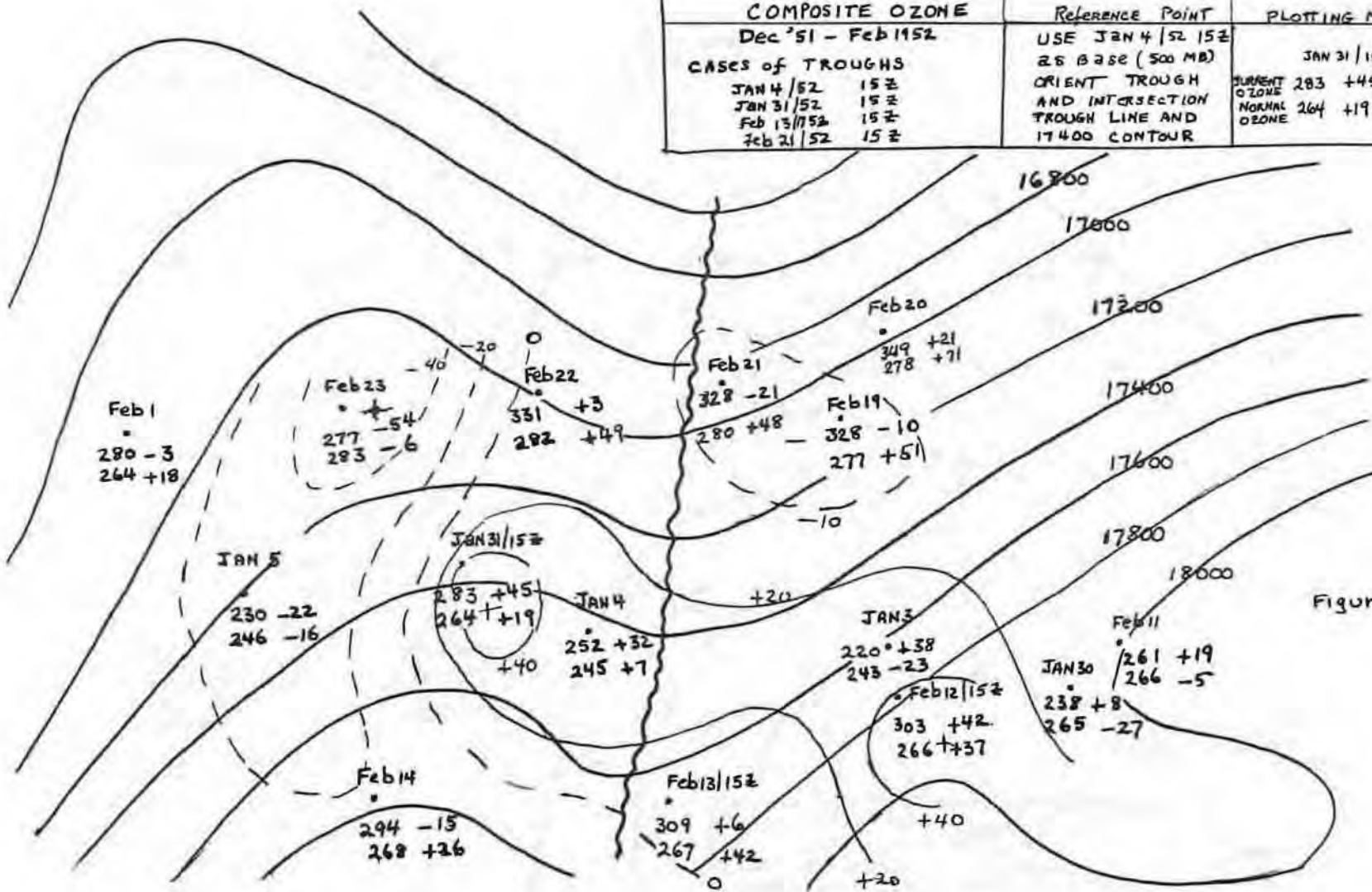


Figure # 3

FIGURE 3

L7

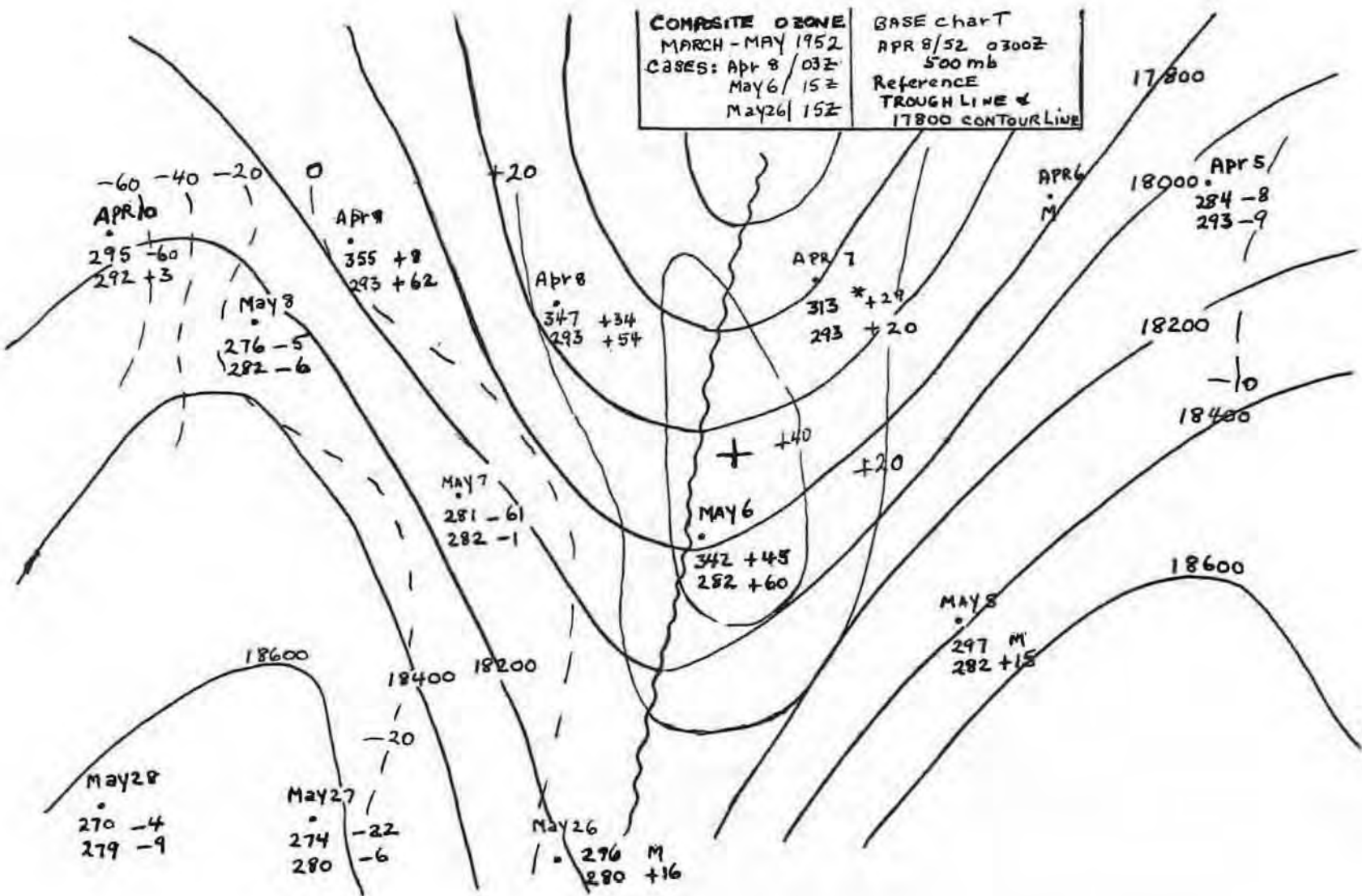


FIGURE 4

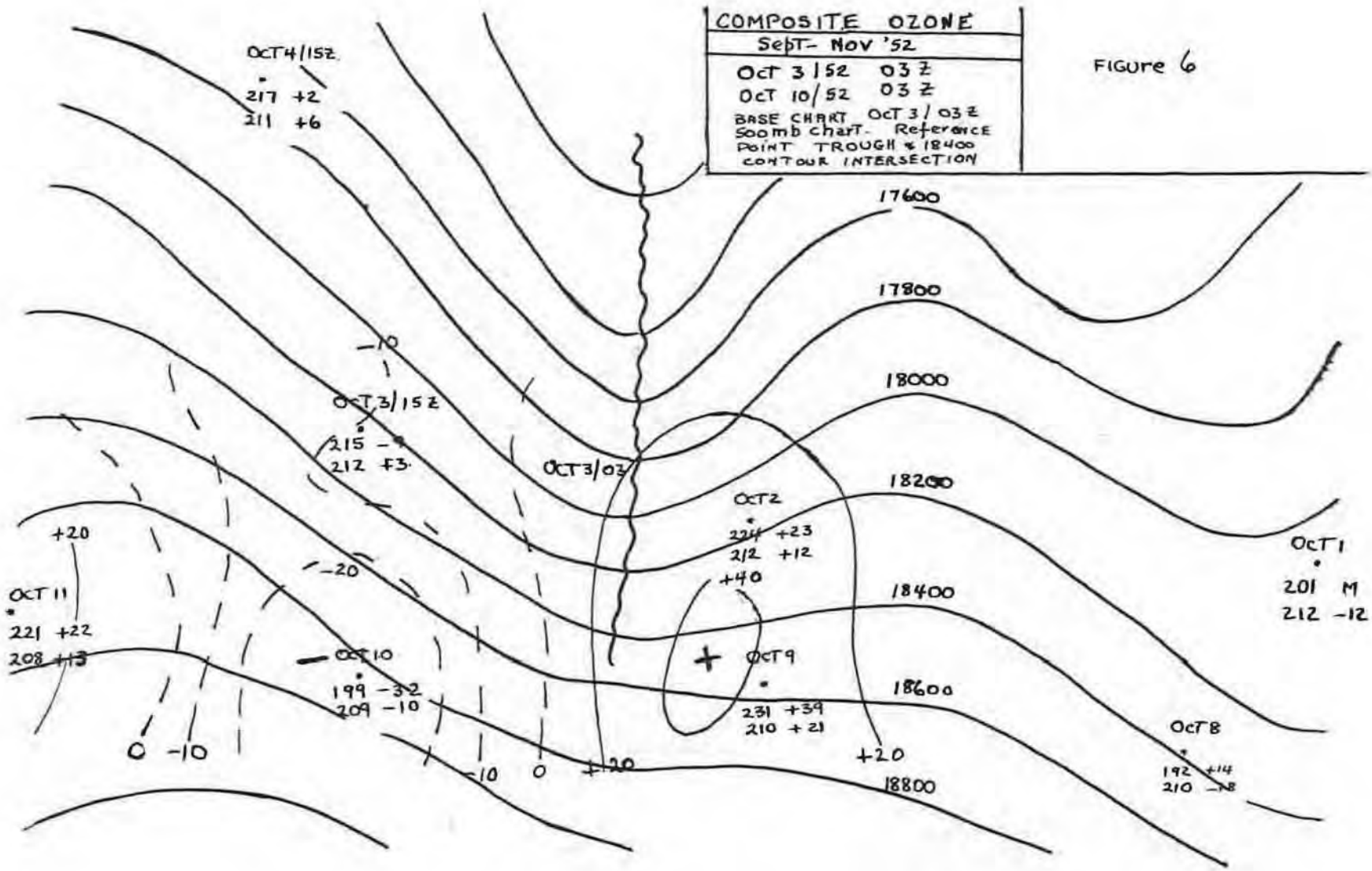


FIGURE 6

FIGURE 6

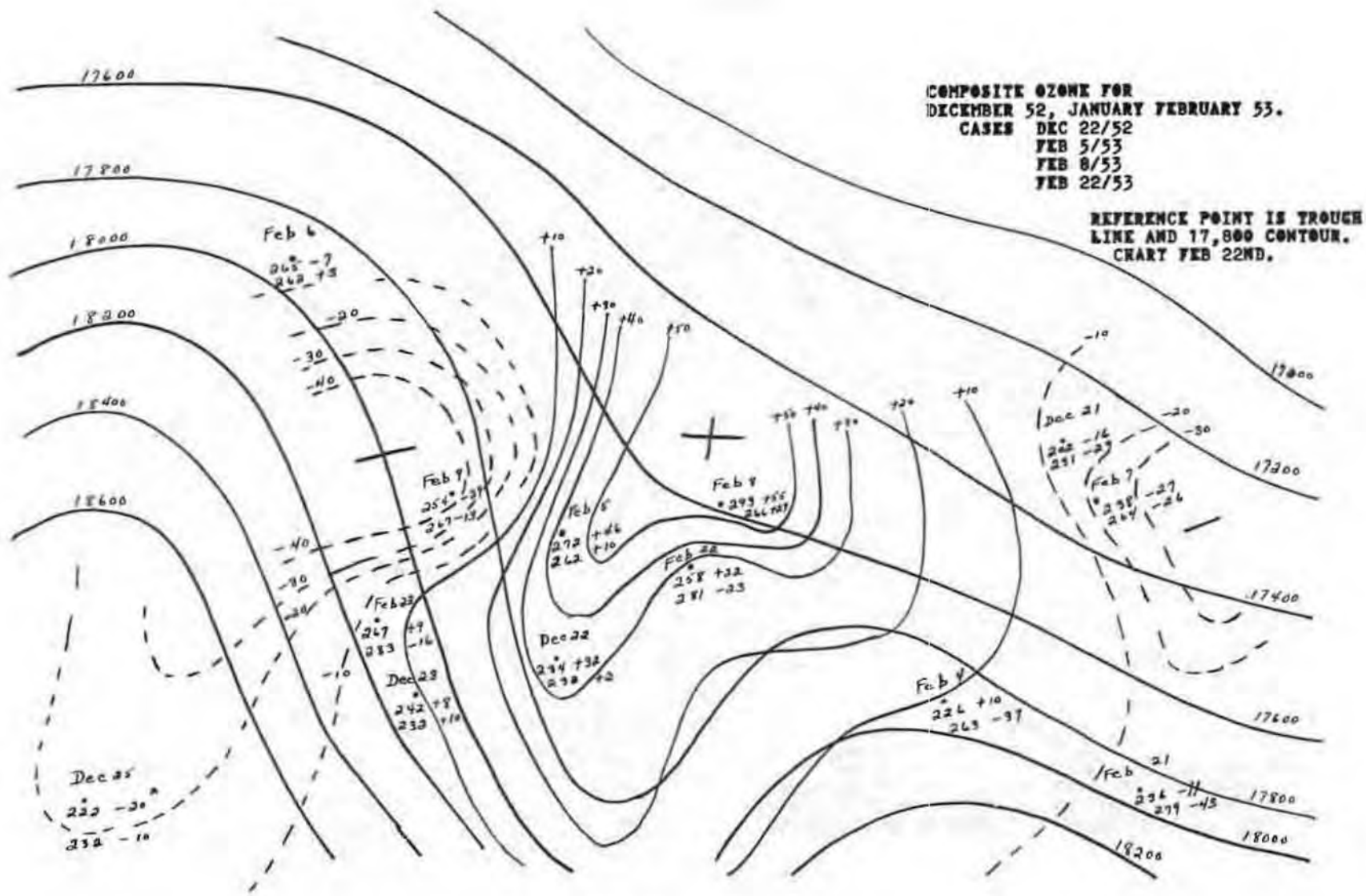
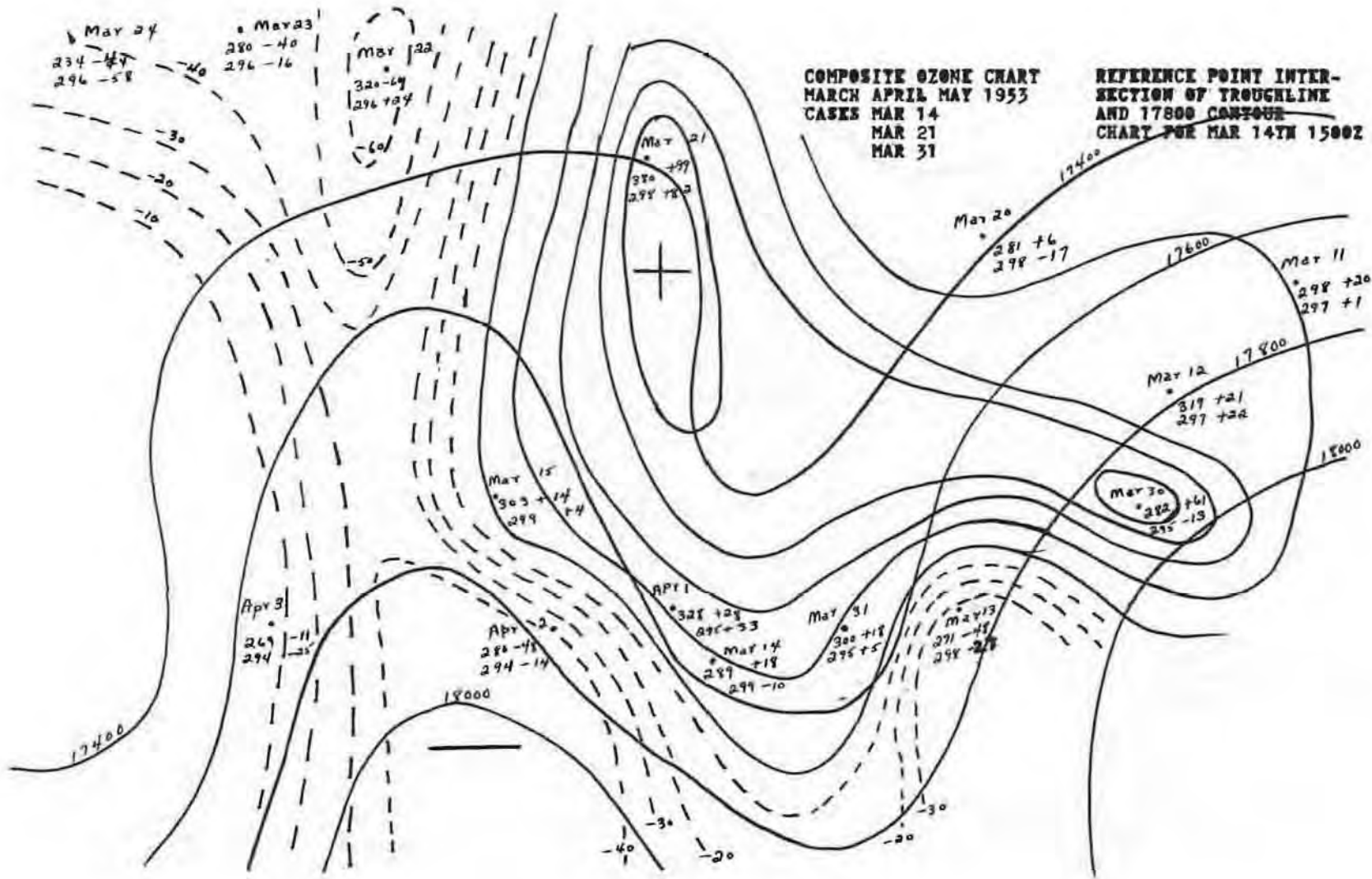


FIGURE 7



COMPOSITE OZONE CHART
 MARCH APRIL MAY 1953
 CASES MAR 14
 MAR 21
 MAR 31

REFERENCE POINT INTER-
 SECTION OF TROUGHLINE
 AND 17800 CONTOUR
 CHART FOR MAR 14TH 1500Z

FIGURE 8

'COMPOSITE' # ZONE
 1 CASE JUNE-AUG/83
 July 15/15z, 1953

PLOTTING MODEL
 CURRENT 297 +35 Tendency
 Smoothed Mean 259 +38 DEVIATION
 anomaly

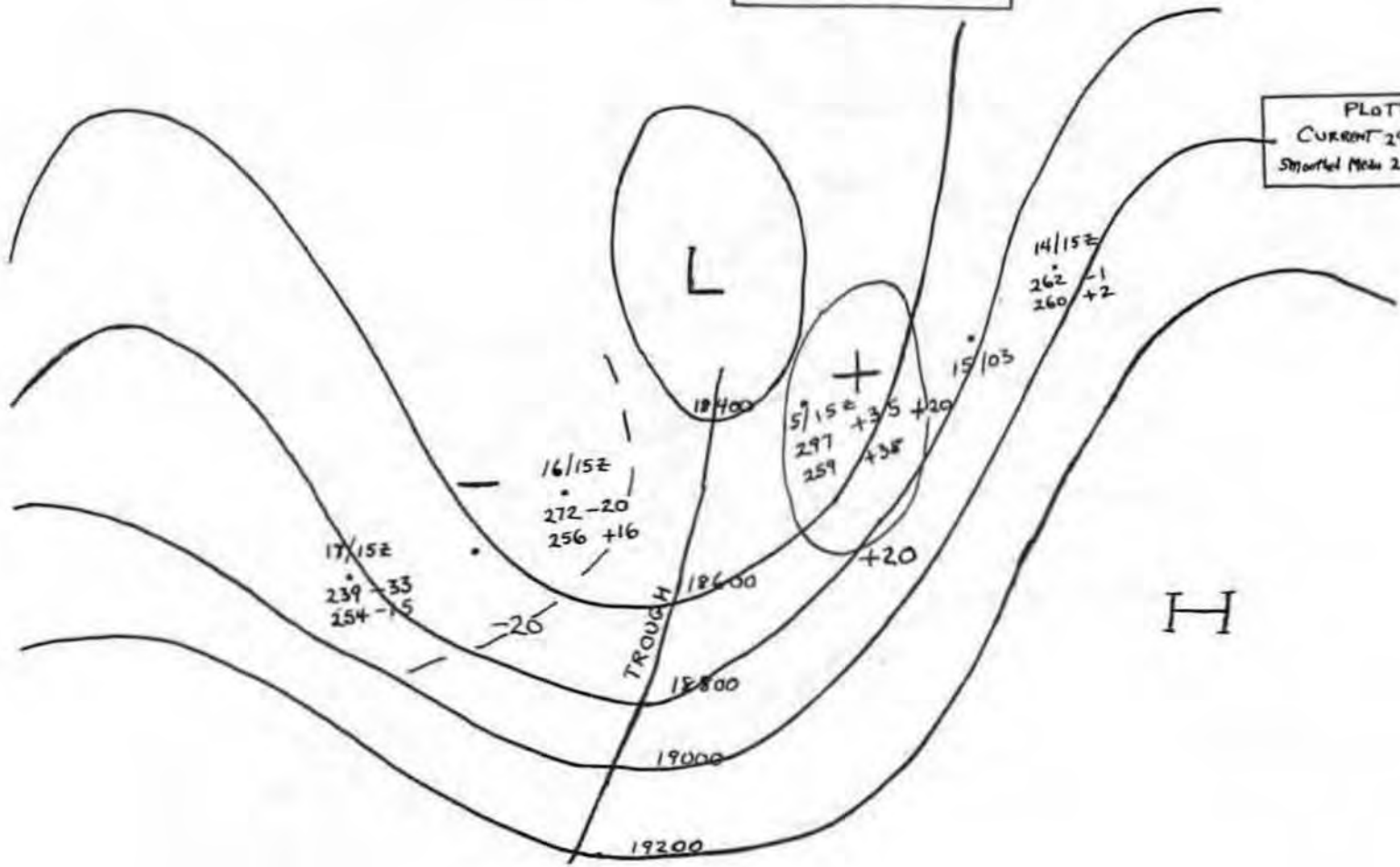


FIGURE 9

COMPOSITE OZONE Sept - Nov 1953	
Sept 2/53	REFERENCE POINT
Sept 17/53	TROUGH LINE
Sept 25	and 18000
Oct 21	CONTOUR
Nov 2	BASIC map 0300Z
Nov 17	OCT 21/53 500 mb

Nov 16
203 +18
212 -9

Nov 18
224 +3
214 +9

Nov 17
221 +18
213 +8

PLOTTING Model
CURRENT OZONE 250 -15 ← TENDENCY
OZONE MEAN → 231 +19 ← ANOMALY

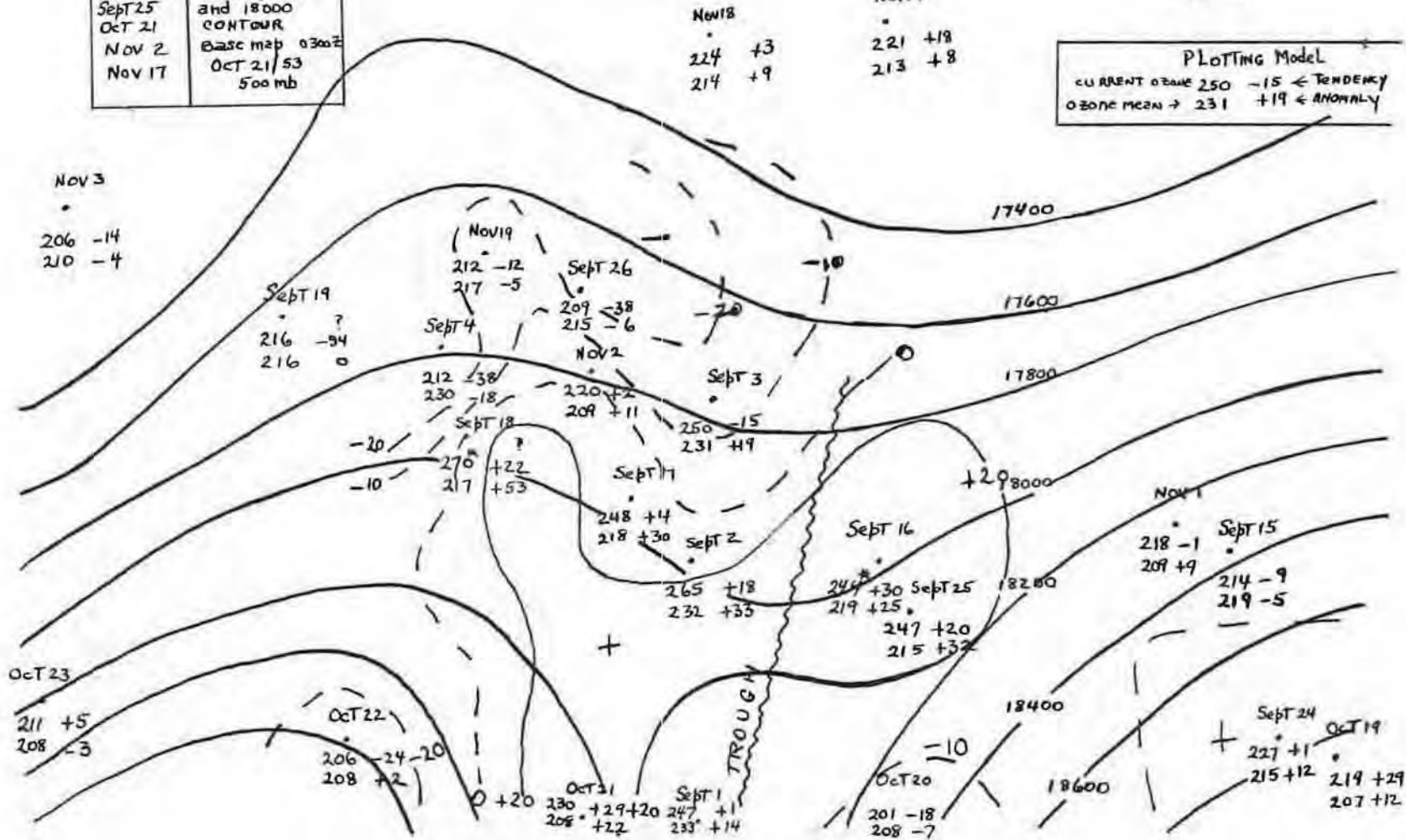
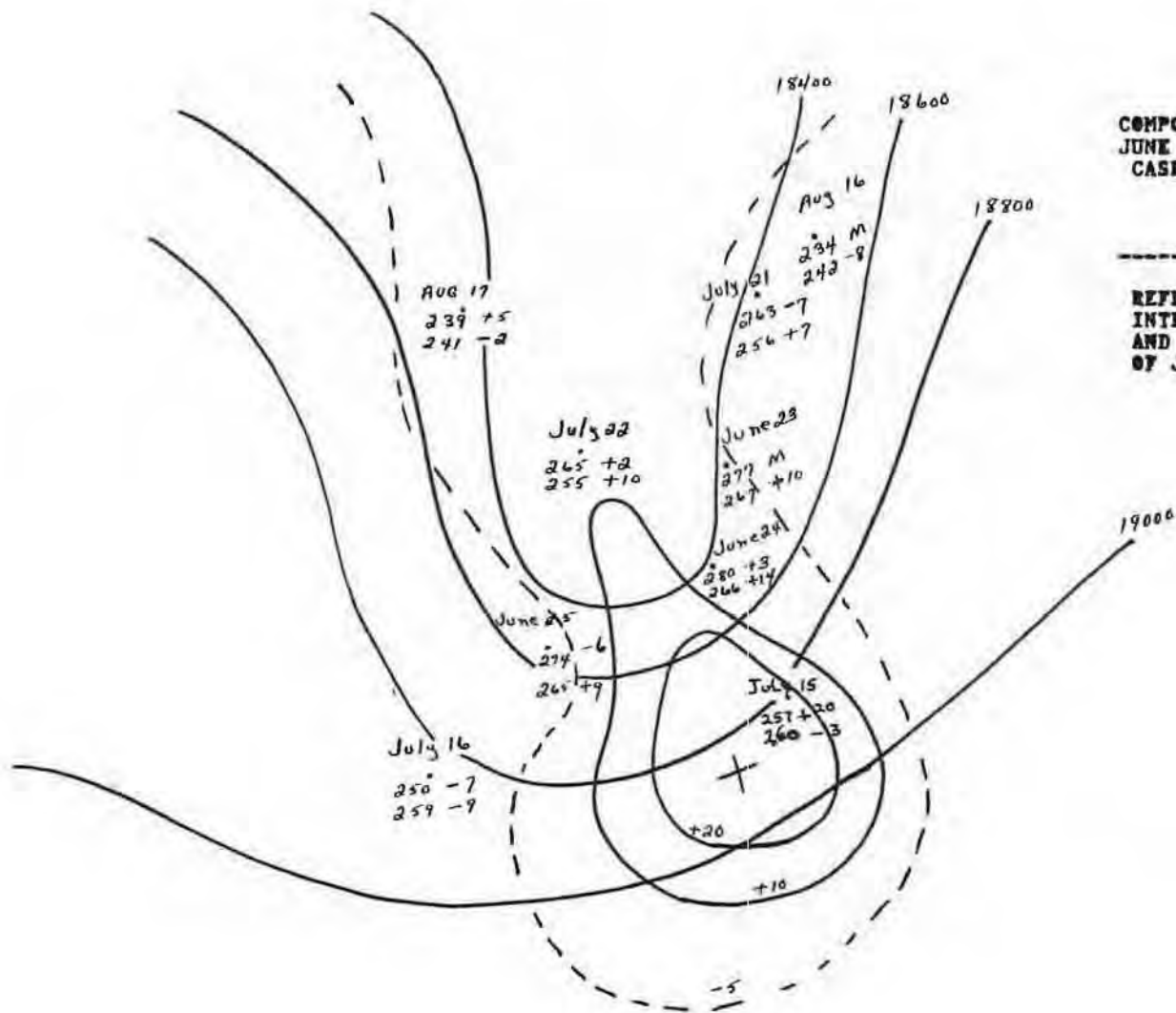


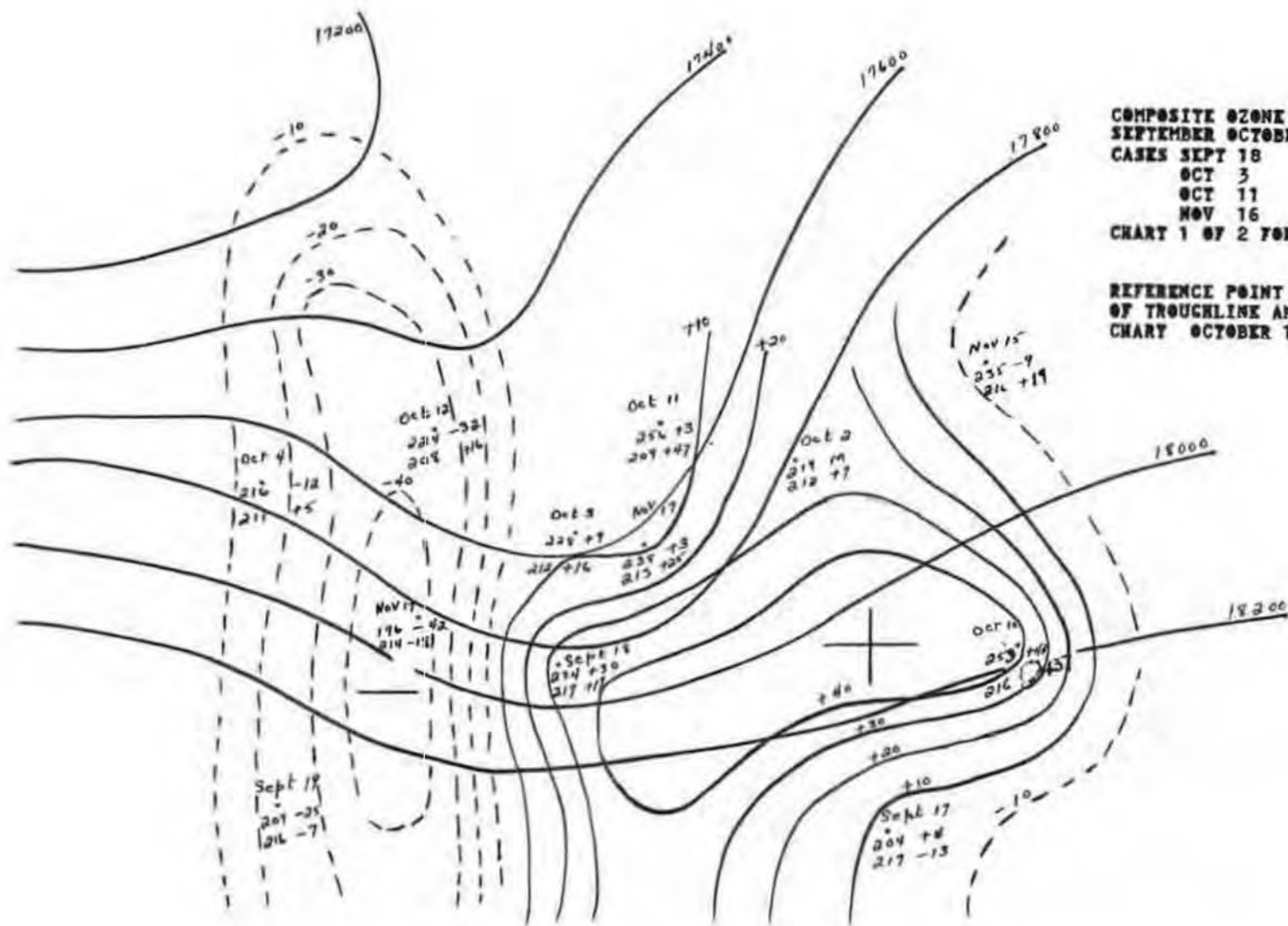
FIGURE 10



COMPOSITE OZONE CHART
JUNE JULY AUGUST 1954.
CASES JUNE 25
 JULY 15
 JULY 21
 AUG 16

REFERENCE POINT
INTERSECTION OF 18,800 CONTOUR
AND TROUGH LINE, USING CHART
OF JULY 21/54 1500Z.

FIGURE 11



COMPOSITE OZONE CHART FOR
 SEPTEMBER OCTOBER NOVEMBER 1954.
 CASES SEPT 18
 OCT 3
 OCT 11
 NOV 16
 CHART 1 OF 2 FOR THIS PERIOD.

REFERENCE POINT IS INTERSECTION
 OF TROUGHLINE AND 17,800 CONTOUR.
 CHART OCTOBER 11TH, 1500Z.

FIGURE 12

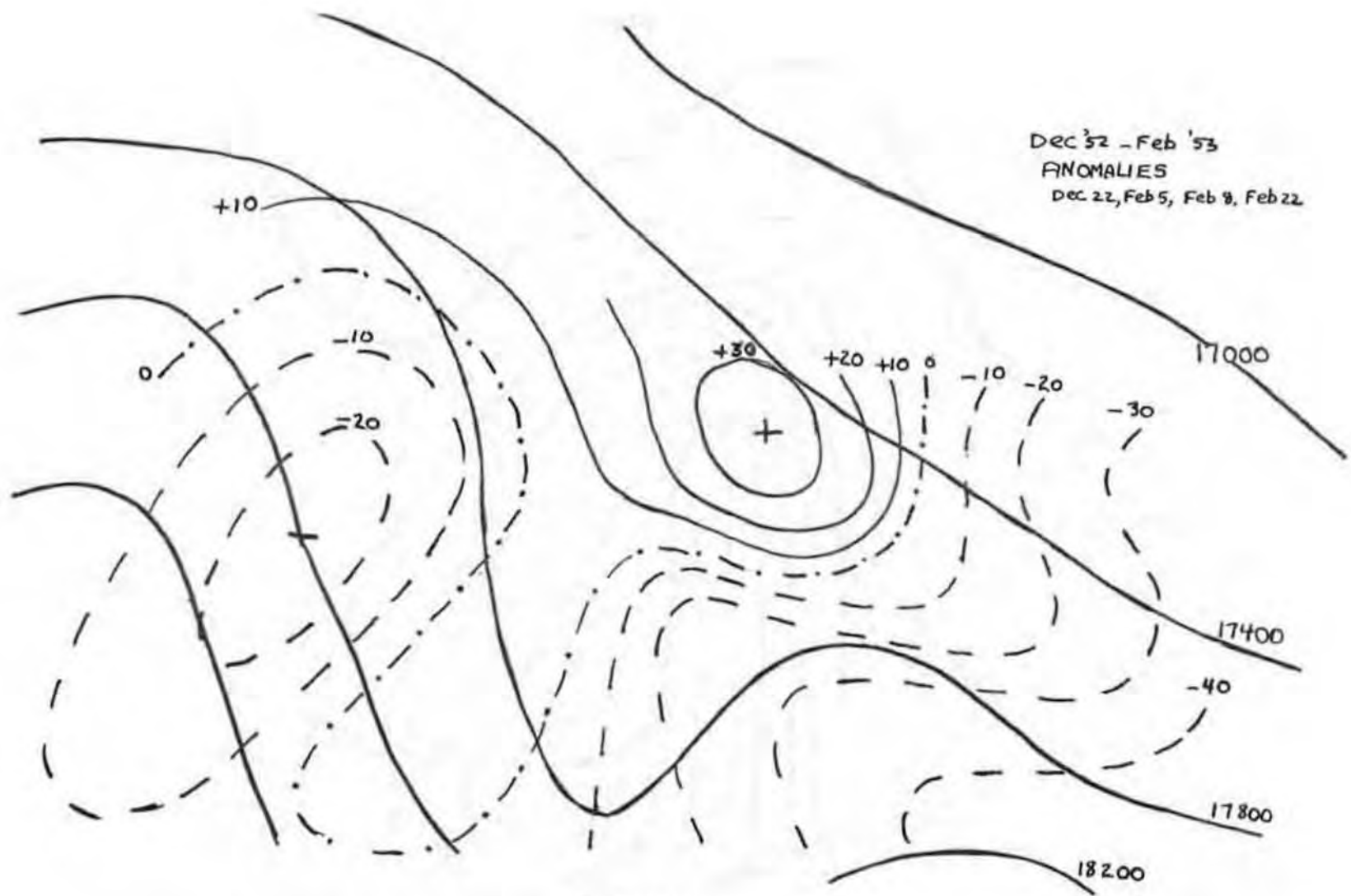


FIGURE 13

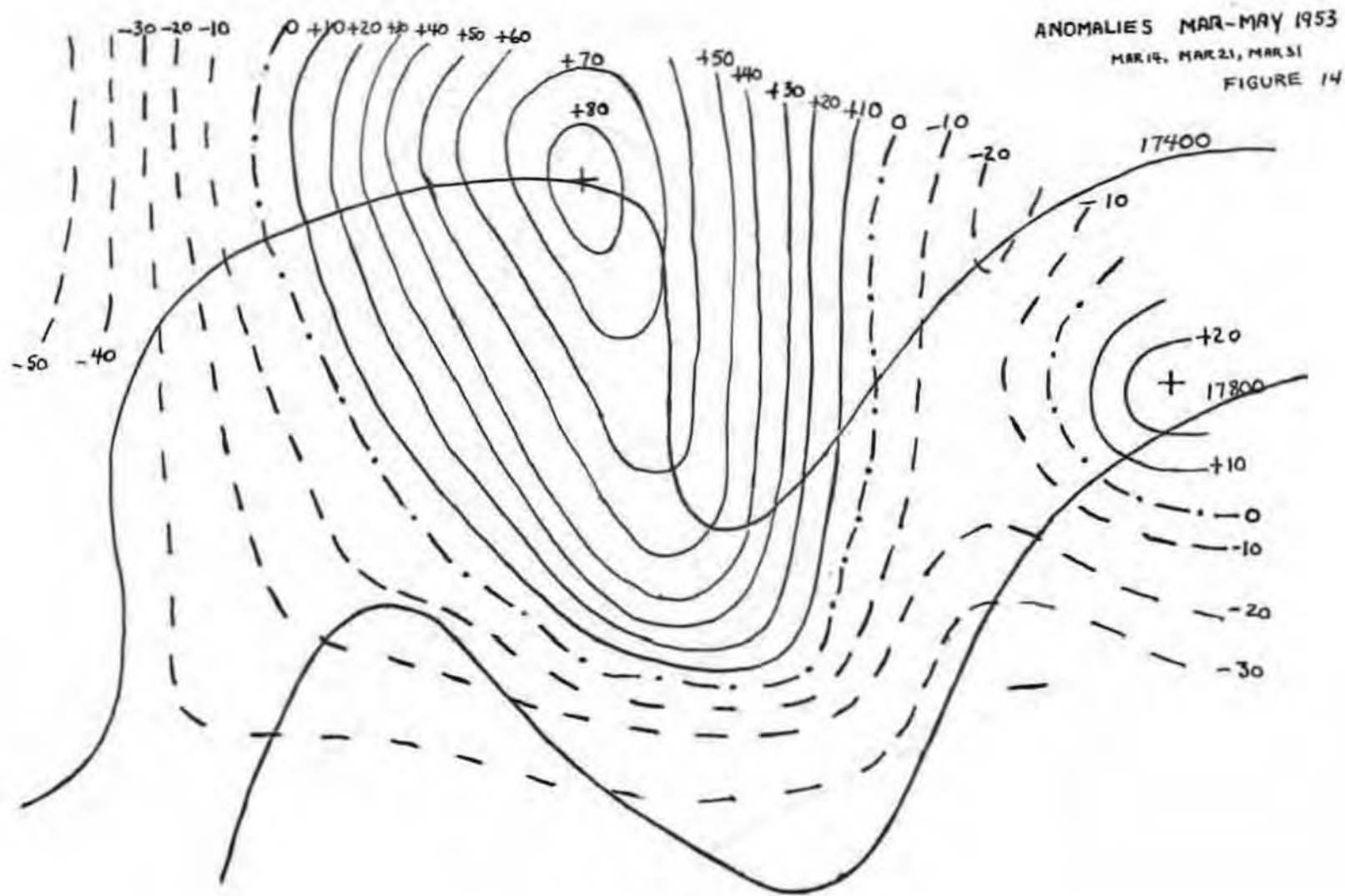


FIGURE 14



Fig 15
 JUNE-AUG 1954
 ANOMALIES
 (ISOPLETHS OF
 DIFFERENCE FROM
 NORMAL OZONE)
 JUNE 25, JULY 15
 JULY 21, AUG 16
 UNITS cm^{-3}

FIGURE 15

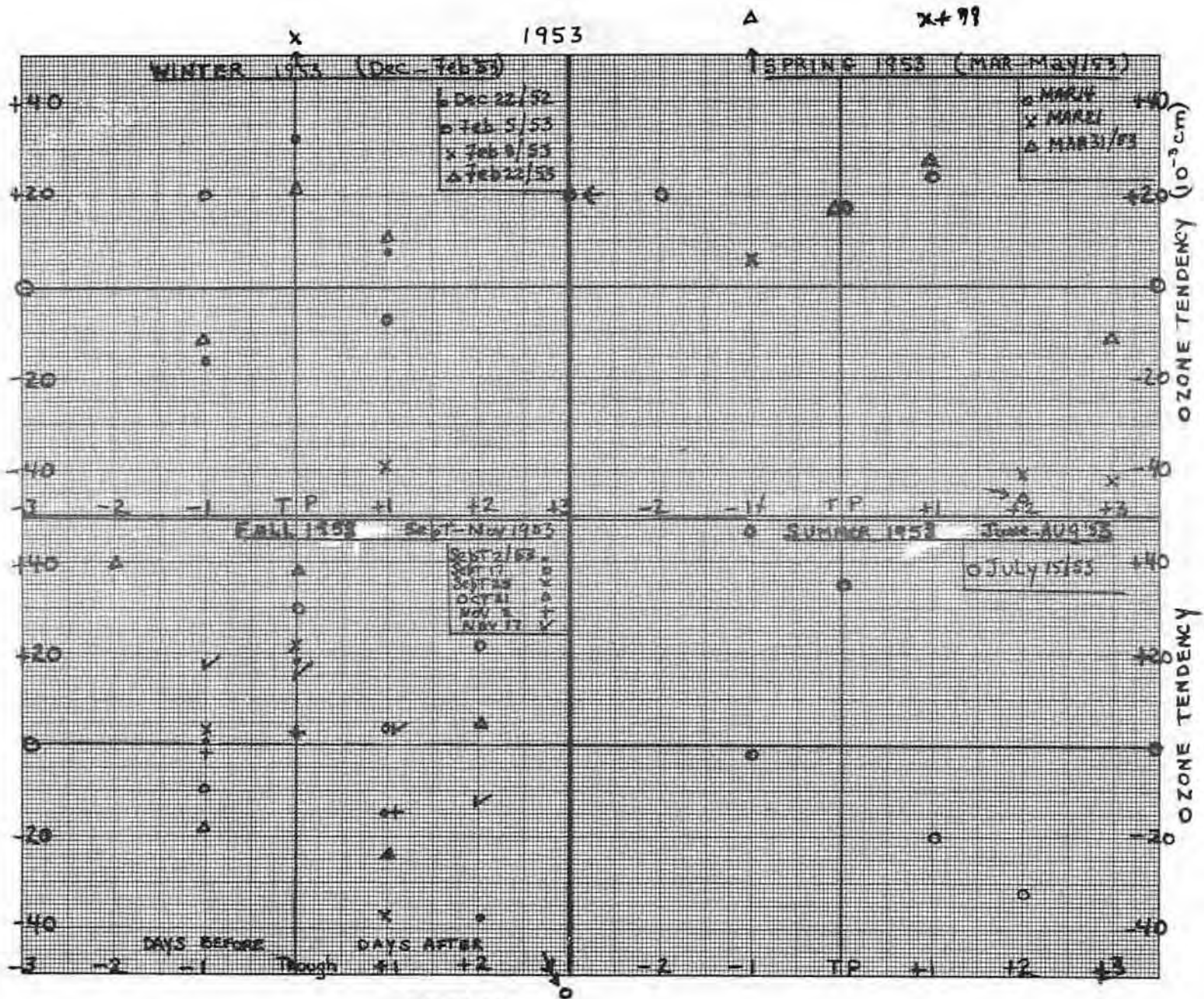


FIGURE 17

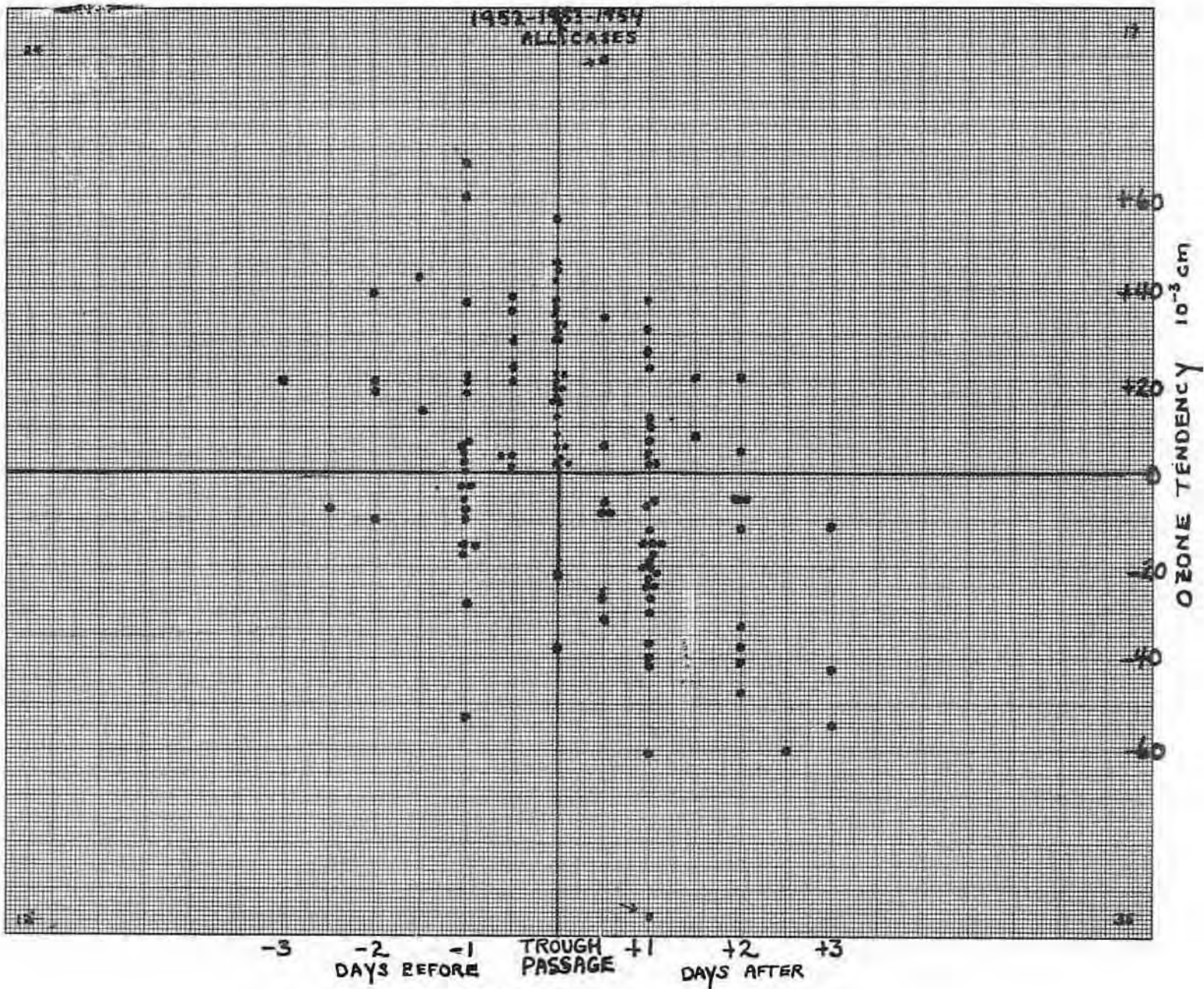


FIGURE 18

BASE MAP Mar 2/52

Plotting Model

OZONE	24hr TENDENCY
MEAN OZONE	DEVIATION from MEAN

Note: very high values

OZONE COMPOSITE COLD LOW HUDSON BAY TYPE

1. Mar 2/52 15Z
2. Nov 20/52 15Z
3. Apr 12/53 15Z
4. July 3/53 15Z

ISOPLETHS of ANOMALY DRAWN

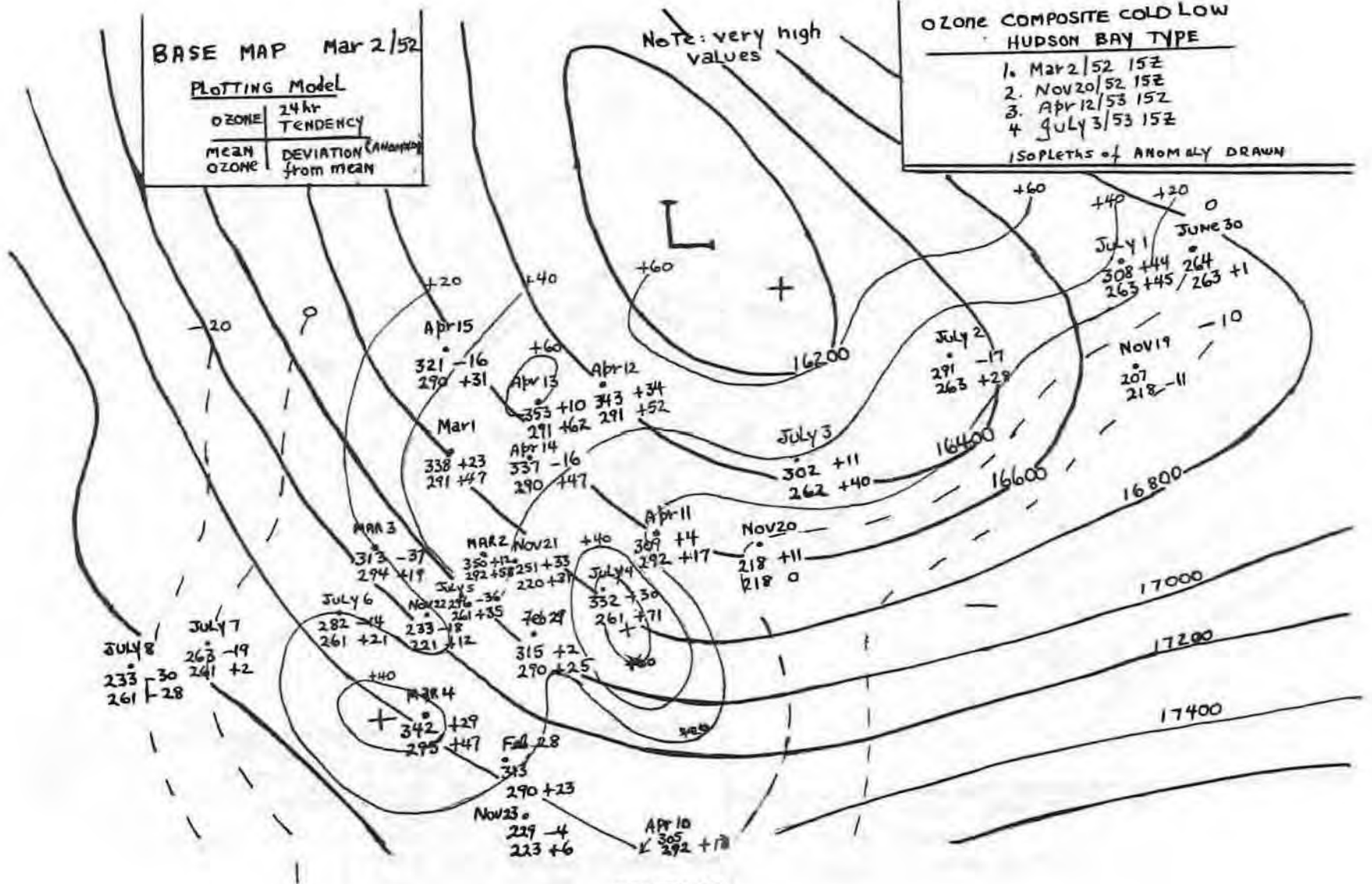


FIGURE 19

PLOTTING Model

CURRENT → 248
 OZONE → 269
 MEAN OZONE → 269

+32 ← 24 hr TENDENCY
 (A means 48 hr)
 -21 ← DEVIATION
 FROM NORMAL
 (ANOMALY)

COMPOSITE OZONE
 COLD LOW - ALBERTA SUMMER TYPE

1. JUNE 14, 52 15Z
2. JUNE 22, 52 15Z
3. MAY 8, 53 15Z
4. AUG 1, 53 03Z
5. AUG 15, 53 15Z

ISOPLETHS OF ANOMALY

ORIENT CENTRE OF LOW AND FIRST
 'OPEN' CONTOUR

BASE MAP JUNE 22/52 15Z

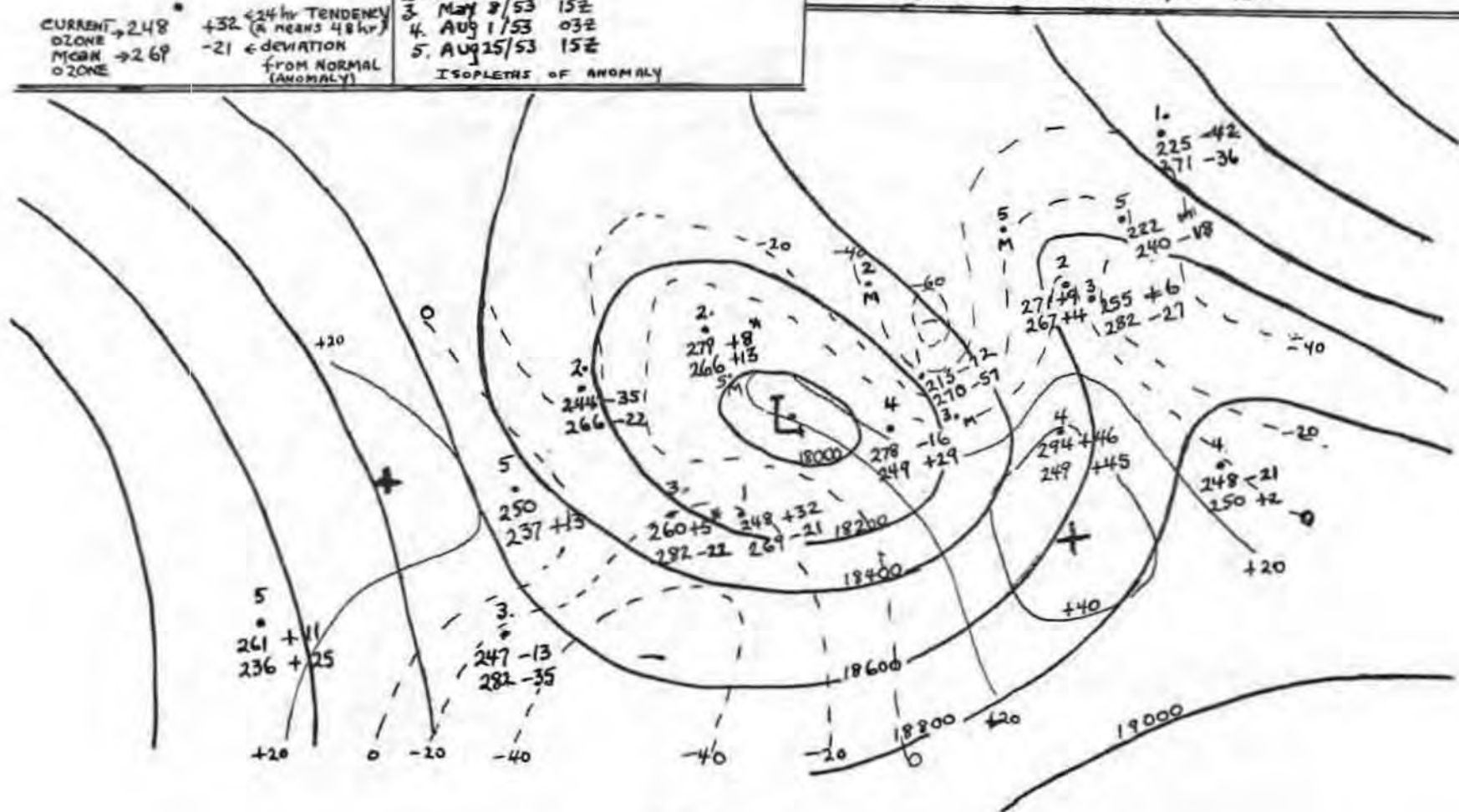


FIGURE 20

<u>Number of Days - 1953.</u>					
Levels of:	100 mb	200 mb	300 mb	500 mb	Trop.
Ozone up, Height down, or vice versa.	119	136	144	139	130
Both up or down.	84	74	71	76	82
No significant change.	15	15	16	21	14
Total Days.	218	225	231	236	226
Fraction Showing Negative Correlation.	.55	.61	.62	.59	.58

TABLE 1